

1

2 **Anthropogenic VOC in Abidjan, southern West Africa: from source** 3 **quantification to atmospheric impacts**

4

5 Pamela Dominutti^{1*}, Sekou Keita ^{2,3}, Julien Bahino^{2,3}, Aurélie Colomb¹, Cathy Liousse², Veronique
6 Yoboué³, Corinne Galy-Lacaux², [Eleanor Morris](#)⁴, Laëtitia Bouvier¹, Stéphane Sauvage⁵ and Agnès
7 Borbon¹

8

9 ¹ Laboratoire de Météorologie Physique LaMP-OPGC-CNRS, Université Clermont Auvergne, Clermont-Ferrand,
10 France

11 ² Laboratoire d'Aérodologie, Université Paul Sabatier Toulouse 3 - CNRS, Toulouse, France

12 ³ Laboratoire de Physique de l'Atmosphère (LAPA)- Université Felix Houphouët-Boigny, Abidjan, Côte d'Ivoire

13 ⁴ [Wolfson Atmospheric Chemistry Laboratories, Department of Chemistry, University of York, Heslington, York,](#)
14 [YO10 5DD, UK](#)

15 ⁵ IMT Lille Douai, Sciences de l'Atmosphère et Génie de l'Environnement (SAGE), Douai, France

16 **Now at [Wolfson Atmospheric Chemistry Laboratories, Department of Chemistry, University of York, Heslington,](#)*
17 *[York, YO10 5DD, UK](#)*

18

19 Correspondence to P. Dominutti (pamela.dominutti@york.ac.uk) + A. Borbon (agnes.borbon@uca.fr)

20

21 **Abstract**

22 Several field campaigns were conducted in the framework of the Dynamics-Aerosol-Chemistry-Cloud Interactions
23 in West Africa (DACCIWA) project to measure a broad range of atmospheric constituents. Here we present the
24 analysis of an unprecedented and comprehensive dataset integrating up to fifty-six volatile organic compounds
25 (VOCs) from ambient sites and emission sources. VOCs were collected on sorbent tubes in the coastal city of
26 Abidjan, Côte d'Ivoire, in winter and summer 2016 and later analysed by gas chromatography coupled with flame
27 ionization and mass spectrometer detectors (GC-FID and GC-MS) in a laboratory.

28 The comparison between VOC emission source profiles and ambient profiles suggests the substantial impact of two-
29 stroke motorized two-wheel vehicles and domestic fires on the composition of Abidjan's atmosphere. However,
30 despite the high VOCs concentrations near-source, moderate ambient levels were observed (by a factor of 10 to 4000
31 lower), similar to the concentrations observed in northern mid-latitude urban areas. Besides photochemistry, the
32 reported high wind speeds seem to be an essential factor that regulates air pollution levels in Abidjan.

33 Emission ratios ($\Delta\text{VOC}/\Delta\text{CO}$) were established based on real-world measurements achieved at a selected number of
34 representative combustion sources. Maximum measured molar mass emissions were observed from two-wheel
35 vehicles (TW), surpassing other regional sources by two orders of magnitude. Local practices like waste burning also
36 make a significant contribution in VOC emissions, higher than those from light-duty vehicles by 1.5 to 8 orders of
37 magnitude. These sources also largely govern the VOCs atmospheric impacts in terms of OH reactivity, secondary

38 organic aerosol formation (SOAP) and photochemical ozone creation potential (POCP). While the contribution of
39 aromatics dominates the atmospheric impact, our measurements reveal the systematic presence of anthropogenic
40 terpenoids in all residential combustion sectors. Finally, emission factors were used to retrieve and quantify VOC
41 emissions from the main anthropogenic source sectors at the national level. Our detailed estimation of VOC emissions
42 suggests that the road transport sector is the dominant source in Côte d'Ivoire, emitting around 1200 Gg yr⁻¹ of gas-
43 phase VOCs. These new estimates are 100 and 160 times larger than global inventory estimations from MACCity or
44 EDGAR (v4.3.2), respectively. Additionally, the residential sector is also largely underestimated in the global
45 emission inventories, by a factor of 13 to 43. Considering only Côte d'Ivoire, these new estimates for VOCs are three
46 to six times higher than the whole of Europe. Given the significant underestimation of VOC emissions from transport
47 and residential sectors in Côte d'Ivoire, there is an urgent need for the whole West African region to build more
48 realistic and region-specific emission inventories. This is not only true for VOCs but for all atmospheric pollutants.
49 The lack of waste burning, fuelwood burning and charcoal representation in regional inventories also needs to be
50 addressed, particularly in low-income areas where these types of activities are ubiquitous sources of VOCs emissions.
51

52 **Keywords: VOCs, emission inventories, West Africa, air pollution, emission ratios.**

53

54 1. Introduction

55 The West Africa region, located to the north of the Gulf of Guinea, is one of the most populated areas in Africa with
56 more than 300 million inhabitants in 2016 (United Nations, 2017). The population has increased by a factor of five
57 since 1950, making West Africa the fastest growing region in the world. Furthermore, future projections indicate
58 population densities in developing countries will increase. The impact in Africa will be particularly high, with
59 projections indicating that the population of the continent could represent 40% of the world's population by 2100
60 (United Nations, 2017). The unplanned explosive growth of urban centres in the region is one of the main issues,
61 with water access, air pollution, health problems and unregulated emissions being identified as major concerns.

62 Consequently, these emissions can produce diverse effects on atmospheric chemistry which are enhanced by severe
63 photochemical conditions and dynamic atmospheric interactions. The atmospheric composition over West Africa is
64 affected by air masses transported from remote sources, i.e., aerosol dust from the Sahara Desert or biomass burning
65 plumes and local urban pollution (Knippertz et al., 2017; Mari et al., 2011). Observations performed during the
66 AMMA (African Monsoon Multidisciplinary Analysis) campaign showed that air quality issues are predominantly
67 related to traffic and combustion emissions (Mari et al., 2011). Residential emissions in Southern West Africa (SWA)
68 are attributed to charcoal and wood burning as they are primary sources of domestic energy, widely used for cooking
69 and heating activities. Biomass burning is a significant source of carbonaceous aerosols and volatile organic
70 compounds (VOCs) that can have effects on public health and climate through the formation of secondary pollutants
71 (Gilman et al., 2015; Knippertz et al., 2015; Sommers et al., 2014).

72 Additionally, in most of the SWA cities, traffic emissions are important sources of air pollution (Assamoi and
73 Liousse, 2010). The road transport sector is largely disorganized due to the underdevelopment of road networks and
74 to the absence of a regulation policy for public transportation (Assamoi and Liousse, 2010). As a result, TW vehicles
75 are widely used in the cities for short-distance travel, replacing public transport. Furthermore, the vehicle fleet has
76 increased in the last year, which is characterized in most cities by a large number of old vehicles (Keita et al., 2018).

77 Over the next few years, African emissions from the combustion of fossil fuels, biofuels and refuse are expected to
78 increase considerably and could represent about 50% of the global emissions of organic carbon (Knippertz et al.,
79 2017; Liousse et al., 2014). Nevertheless, the emission estimates are uncertain and detailed emission inventories are
80 still required for a better estimation of their impacts on climate change and health over this highly sensitive region
81 (Knippertz et al., 2017).

82 VOCs include a large number of species which can affect air quality by producing secondary pollutants such as ozone
83 and secondary organic aerosols (Seinfeld and Pandis, 2006). Given the reactive nature of VOCs (Atkinson and Arey,
84 2003a), their emissions need to be disaggregated by species or species groups for a better representation of their
85 chemical features, and to assess their impacts on the secondary formation processes. As VOCs are important
86 pollutants present in urban atmospheres, in-situ VOC observations are necessary to directly assess exposure and to
87 improve the prediction of secondary products formation.

88 Several field campaigns have been conducted in the last twenty years all over the world with the purpose of
89 characterizing VOC species for a better understanding of their emission sources and fate (Bechara et al., 2010; Bon
90 et al., 2011; Borbon et al., 2013; Brito et al., 2015; Dominutti et al., 2016; Kumar et al., 2018; Salameh et al., 2015;
91 Wang et al., 2014; Warneke et al., 2016). In particular, VOC field observations have also been intensely used as
92 constraints for the development of reliable emission inventories (Borbon et al., 2013; Boynard et al., 2014; Gaimoz
93 et al., 2011; Niedojadlo et al., 2007; Salameh et al., 2016b). Some of these studies pointed out significant
94 discrepancies between inventory estimations and emission ratios derived from ambient measurements, implying
95 some limitations in the accurate modelling of VOCs impacts. For the only northern mid-latitude cities, discrepancies
96 up to a factor of 10 for VOCs emissions were observed (Borbon et al., 2013; Boynard et al., 2014). Such discrepancies
97 are expected to be even more substantial in sensitive places with high anthropogenic pressures like Africa and South
98 America (Huang et al., 2017). For Africa in particular, the emission inventories frequently used are those developed
99 for global scales due to the lack of observations, which involves numerous uncertainties (Keita et al., 2018; Liousse
100 et al., 2014). The main differences between emission inventories and source emissions are associated with the
101 emission source estimations due to a lack of VOC speciation and spatiotemporal characterization.

102 Furthermore, global emission inventories commonly estimate the total mass of VOCs. However, the fate and
103 contribution of each species can change depending on the emission source, fuel quality, combustion technologies,
104 and main regional activities (Huang et al., 2017). The use of activity data and emission factors derived from local
105 measurements of regional-specific sources may help to reduce the uncertainties in these emission inventories. A
106 recent study calculated the emission factors (EFs) of different compounds and activities in SWA (Keita et al., 2018).
107 A comparison of the emissions calculated from the EFs with those observed from the EDGARv4.3.2 (Huang et al.,
108 2017) inventory showed a marked discrepancy (factor of 50 difference) for fifteen VOCs species (3 alkanes, 8
109 aromatics, isoprene and 3 monoterpenes) in Côte d'Ivoire. This work has emphasised the importance of considering
110 African anthropogenic emissions at regional scales. Due to the scarcity of suitable data the uncertainties in the
111 observations cannot currently be assessed and more detailed studies are required to quantify these uncertainties.
112 Characterization and quantification of the emissions is crucial for improving our understanding of the contributions
113 of anthropogenic and natural sources to the atmospheric composition over SWA, and for assessing their impact on
114 public health and air quality conditions.

115 Several intensive field campaigns in the framework of the Dynamics-Aerosol-Chemistry-Cloud-Interactions in West
116 Africa (DACCIWA) project were conducted in 2015 and 2016 (Knippertz et al., 2015). Here, we present the results
117 obtained from the VOC field campaigns at different sites, including ambient and near-source measurements, in one
118 of the major SWA cities: Abidjan in Côte d'Ivoire. Speciated VOCs were collected off-line using sorbent tubes, and
119 then analysed and quantified at the laboratory applying different gas chromatography techniques. These data provide
120 the first constraints for the construction of a regional emission inventory and for understanding the role of
121 anthropogenic VOC emissions in the regional atmospheric chemistry.

122 This work aims to establish and analyse the spatial distribution of VOC concentrations and VOC speciated profiles
123 of primary anthropogenic sources in Abidjan by performing sampling in real-condition operation. These sources
124 include traditional and regional-specific ones, such as road transportation (gasoline, diesel, and TW emissions),
125 charcoal fabrication and burning emissions from domestic cooking fires, landfill waste, and hardwood fuel. This new
126 dataset provides substantial information enabling the quantification of VOC emissions for several sources in Côte
127 d'Ivoire. These source profiles are analysed and contrasted with those provided by global emission inventories.
128 Finally, the impact on air quality due to the use of regional-specific sources is assessed in terms of reactivity and
129 secondary pollutant formation.

130

131 **2. Materials and Methods**

132 As part of the DACCIWA project, intensive field campaigns were performed in 2015 and 2016, focusing for the first
133 time on the most populated southern coastal region of West Africa. The DACCIWA campaign had an emphasis on
134 atmospheric composition, including air pollution, health impacts and cloud-aerosol interactions (Knippertz et al.,
135 2015). Here we present new results from intensive ambient measurements in Abidjan and an extended VOC
136 speciation from source emission measurements. These results are part of the activities developed under the work
137 package 2 (WP2) - Air pollution and Health - which aims to link and quantify emission sources, air pollution and
138 related health impacts over different urban sources in West Africa.

139 Abidjan is the economic capital of Côte d'Ivoire with a population of 6.5 million (in 2016), representing more than
140 20 percent of the overall population of the country (United Nations, 2017). Along with autonomous districts, Abidjan
141 encompasses an area of 2119 km² and is distinguished by remarkable industrialization and urbanization. In summer,
142 West Africa is influenced by monsoon phenomenon which is mainly driven by the surface pressure contrast between
143 the relatively cold waters of the tropical Atlantic Ocean and the Saharan heat low (Knippertz et al., 2017). This
144 seasonal circulation characterized the wet (summer) and dry (winter) periods in the region. During the dry season
145 (November to February), most of the region is dominated by dry north-easterly winds from the Sahara and the
146 precipitation is confined to the coast, where the sea-breeze circulation provides humid air and produces near-surface
147 convergence. Then, the monsoon starts its development and south-westerly moist winds begin to enter deeper into
148 the continent producing more clouds and precipitation between July and August. The strong pressure and temperature
149 gradients between the Atlantic Ocean and the Sahara drive the strong monsoon flow northward along with south-
150 westerlies, reaching higher latitudes up to 20° N (Knippertz et al., 2015).

151

152

153

154 2.1 Sampling

155 The field campaigns were conducted in Abidjan, Côte d'Ivoire during summer and winter according to the strategic
156 directions of the DACCIWA WP2. Cartridges deployed for VOC measurements were composed of Tenax TA 60-80
157 mesh (250 mg) or Carbopack C (150 mg). The combination of both sorbent materials allowed the sampling of 10
158 aromatics (C6-C9), 22 n-alkanes (C5-C16), 10 monoterpenes, 7 aldehydes, isoprene, and other oxygenated
159 compounds. All compounds are reported in Table S1. Before the sampling, multi-sorbent filled cartridges were
160 conditioned by flowing purified nitrogen through them, at a rate of 100 mL min⁻¹, during 5 hours at 320 °C.

161 Firstly, ambient VOC were collected to analyse their spatial distribution in Abidjan. Ambient measurements were
162 performed at nine sites, which are shown in Figure 1. The distribution of the sampling locations was selected
163 according to the primary source locations. They include background sites and areas impacted by residential, road
164 transport, domestic fires, waste burning and industrial activities. The characteristics and geographical location of
165 each site are reported in Table 2. The ambient campaigns were conducted during the dry season (February 2016).
166 Samples were collected every 2 days at different times of the day (from 6 a.m. to 8 p.m.) by using a manual pump
167 (Accuro 2000, Dräger) at 100 mL sccm flow rate. One single sorbent tube was exposed six times at each sampling
168 location. In total, 3.6 L of air were collected at each site for a single 600 mL-volume each time.

169 Secondly, direct source emission measurements were performed to obtain VOC emission profiles from the main
170 anthropogenic sources in Abidjan. The sources include traditional ones like road transportation, and SWA regional-
171 specific ones such as domestic waste-burning, charcoal fabrication, charcoal-burning as well as fuel wood-burning
172 (Table 1). Part of these measurements for a limited number of VOC (fifteen species including 3 alkanes, 8 aromatics,
173 3 terpenes and isoprene), BC and particles were already discussed in a recently published paper (Keita et al., 2018).

174 – For road transportation, analysis of different vehicle exhaust measurements was carried out. Samples
175 integrate five road transportation sub-categories: heavy-duty diesel vehicles (HDDV, trucks, and buses – 6
176 samples on Tenax and Carbopack tubes), light-duty diesel vehicles (LDDV, diesel cars, 4 samples on Tenax
177 tubes), light-duty gasoline vehicles (LDGV, gasoline cars, 4 samples on Tenax tubes), two-wheel two-stroke
178 (TW 2T, 6 samples on Tenax and Carbopack tubes) and two-wheel four-stroke (TW 4T, 4 samples on Tenax
179 and Carbopack tubes) vehicles. Differences in fuel type (gasoline and diesel) and the fleet age have been
180 considered. In African countries, two-wheeled vehicles (two-stroke or four-stroke engines) frequently use a
181 mixture of oil and gasoline derived from smuggling, which is characterized by high pollutant emissions
182 (Assamoi and Lioussé, 2010).

183 – Regarding domestic waste-burning (WB), samples were obtained (5 samples on Tenax tubes) at the official
184 domestic landfill site located to the east of Abidjan (AD, Figure 1 and Table 2). The sampling was performed
185 inside the waste burning plume to integrate the different combustion processes involved.

186 – Charcoal-burning (CH) and fuel wood-burning (FW) are common cooking and heating practices in African
187 urban areas. FW emissions were obtained by measuring the fire plume of tropical African hardwood,
188 specifically Hevea (*Hevea brasiliensis*). FW and CH were burned in two types of stoves traditionally used
189 in the SWA region for cooking, which are made of metal and baked earth. The measurements included all
190 the combustion phases (Keita et al., 2018) (3 samples on Tenax and Carbopack tubes).

191 – The charcoal-making (CHM) profile was obtained by measuring emissions from traditional kilns, that use
192 different types of dense wood. The kiln was covered with a layer of leaves and another one of soil of about

193 10 cm thickness. The smoke was sampled through holes made in the CHM kiln, which are located in the
194 horizontal plane, and provide the air circulation for the pyrolysis propagation (Keita et al., 2018) (2 samples
195 on Tenax and Carbopack tubes).

196 All samples were obtained in the emission plume at around 1–1.5m from the source, except for vehicles where
197 samples were taken at the tailpipe outlet while the vehicle's engine was idling. Carbon monoxide (CO) and carbon
198 dioxide (CO₂) measurements were also performed on the emission sources together with the VOC measurements.
199 For this, the QTRAK-7575 sensor (TSI, Keita et al., 2018) was used to measure real-time CO₂ and CO gas
200 concentrations. CO is measured by using an electrochemical sensor with a sensitivity of 0 to 500 ppm with ±3%
201 accuracy. CO₂ concentrations are obtained by using a non-dispersive infrared detector with a sensitivity of 0 to 5000
202 ppm with an accuracy of ±3 %. The instrument was calibrated in the laboratory prior to each emission measurement
203 These concentrations were used for the estimation of EF values from different samples, which were later averaged
204 for every source category.

205

206 *2.2 Analytical instrumentation*

207 Duplicate measurements were performed and analysed in two different laboratories to investigate the reproducibility
208 of analytical techniques and to acquire a wider range of VOC species. The analysis of the Tenax TA tubes was
209 performed at the *Laboratoire de Météorologie Physique* (LaMP, Clermont-Ferrand, France) using a gas
210 chromatograph mass spectrometer system (GC/MS, Turbomass Clarus 600, Perkin Elmer®) coupled to automatic
211 thermal desorption (Turbomatrix ATD). Each tube was desorbed at 270 °C during 15 min at a flow rate of 40 mL
212 min⁻¹ and pre-concentrated on a second trap, at -30°C containing Tenax TA. After the cryofocusing, the trap was
213 rapidly heated to 300°C (40°. s⁻¹) and the target compounds were flushed into the GC. Due to the high loads in some
214 samples, an inlet and outlet split of 5 mL min⁻¹ and 2 mL min⁻¹ were set up, respectively. The analytical column was
215 a PE-5MS (5% phenyl – 95% PDMS, 60m×0.25mm×0.25µm) capillary column (Perkin Elmer) and a temperature
216 ramp was applied to guarantee the VOCs separation (35°C for 5 minutes, heating at 8°C min⁻¹ to 250°C, hold for 2
217 minutes). The mass spectrometer was operated in a Total Ion Current (TIC) from 35 to 350 m/z amu. Chromatography
218 parameters were optimized to enable good separation of fifteen identified compounds by a complete run of 34
219 minutes on each cartridge. Calibration was performed by analysing conditioned cartridges doped with known masses
220 of each compound, present in certified standard low-ppb gaseous standard, purchased from the National Physical
221 Laboratory (NPL, UK). The cartridges were then analysed with the method described above and calibration curves
222 were obtained for each compound as already discussed in Keita et al., (2018). The method provided the separation
223 and identification of 16 compounds, from C5 to C10 VOCs, including 8 aromatics, 3 monoterpenes, 4 alkanes and
224 isoprene.

225 Carbopack tubes analysis was carried out by applying a gas chromatography-flame ionization detector (ATD-GC-
226 FID, Perkin Elmer) system at the *SAGE Department (IMT Lille Douai)*. The cartridges were previously thermo-
227 desorbed at 350 °C for 15 minutes with a helium flow of 20 mL min⁻¹. This method allowed the separation and
228 identification of up to 56 compounds, from C5–C16 VOCs, including 7 carbonyls, 4 ketones, 10 monoterpenes and
229 6 VOCs of intermediate volatility. More details of this technique can be found elsewhere (Ait-Helal et al., 2014;
230 Detournay et al., 2011). The application of both methods allowed the comparison of common compounds that were
231 measured at ambient sites and sources (benzene, toluene, ethylbenzene, m+p-xylene, o-xylene, trimethylbenzenes,

232 n-heptane, iso-octane, n-octane, α -pinene, β -pinene, limonene, isoprene) and the performance analysis of the
233 analytical techniques. Furthermore, the combination of different sorbent tubes and analytical strategies allowed the
234 quantification of a higher number of VOC species, and therefore, a more extensive analysis of source contributions.
235 The detection limits, uncertainties and quality control parameters for both analytical methods can be found elsewhere
236 (Detournay et al., 2011; Keita et al., 2018)

237

238 2.3 Metrics and calculations

239 Different calculations were implemented to assess the VOC emissions and their impacts in Abidjan. Here we provide
240 the equation basis for each investigated parameter. Firstly, the emission factors (EF) were computed for the whole
241 extended VOC database (56 compounds) following the methodology described in Keita et al. (2018). EFs combined
242 with regional statistics were later used for the estimation of VOC emissions in Côte d'Ivoire for each source category.
243 Secondly, the emission ratios (ER) of each VOC species related to CO for all the emission sources were established.
244 Finally, the reported ERs were used to evaluate the impacts on atmospheric reactivity by applying commonly used
245 metrics.

246

247 2.3.1 Emission factors and quantification of VOC emissions

248 VOC emission factors were estimated from the concentrations measured for all the emission sources, as follows

$$249 \quad EF(VOC) = \frac{\frac{\Delta VOC}{\Delta CO} \times MW_{VOC}}{12} \times fc \times 10^3 \quad (1)$$

250 where EF (VOC) is the emission factor of the specific VOC in gram per kilogram of burned fuel (g kg^{-1}); $\Delta VOC =$
251 $[VOC]_{\text{emission}} - [VOC]_{\text{background}}$ is the VOC mixing ratio in the emission and background air respectively, in
252 parts per billion by volume (ppbv); MW_{VOC} is the molar weight of the specific VOC (in g mol^{-1}), 12 is the molar
253 weight of carbon (g mol^{-1}) and fc is the mass fraction of carbon in the fuel analysed. The fc values used were obtained
254 from the literature and applied to each source. The EF for fifteen VOCs were already published and more details
255 about the method can be found elsewhere (Keita et al.; 2018). Here we applied the same method for the whole VOC
256 database.

257 The VOC emissions were estimated from our measurements considering the **expanded** dataset of 56 compounds. For
258 this, VOC emissions were estimated using the emission factors obtained from near-source measurements along with
259 the statistical International Energy Agency (IEA) activity data, available for the different sources (Keita et al., 2018).
260 Equation 1 was used to compute the emission factors, considering all the VOC species measured and including the
261 mass fraction of each fuel (fc) obtained from the literature. Additionally, the differences in fuel type and the fleet age
262 have been considered, as well as the fleet distribution by calculating the equivalent vehicular fleet as described in
263 Keita et al. (2018). For the road transport sector, the equivalent fleet means were calculated considering the fleet
264 characteristics in Côte d'Ivoire, as detailed in Keita et al. (2018). These calculations were based on the information
265 given by the Direction Generale des Transports Terrestres in Côte d'Ivoire, which considered that 60% of vehicles
266 are old models and 77% of the total fleet is composed by light-duty vehicles. Regarding TW, 60% of them are two-
267 stroke engines and only 40% of the total are considered as recent vehicles (SIE CI, 2010). In the residential profile,
268 we integrated the emissions measured from CH, CHM and FW sources, commonly observed at residential sites in
269 Abidjan. Afterwards, the mean road transportation and residential profiles for Côte d'Ivoire were computed and

270 compared with two referenced global inventories, EDGAR v4.3.2 and MACCity (Granier et al., 2011; Huang et al.,
271 2017).

272

273 2.3.2 Molar mass emission ratios

274 Emission ratios (ER) were obtained by dividing each VOC mixing ratio by carbon monoxide (CO) mixing ratios as
275 follows:

$$276 \quad ER = \frac{[VOC] \text{ ppbv}}{[\Delta CO] \text{ ppmv}} \quad (2)$$

277 We selected CO as a combustion tracer because most VOCs and CO are co-emitted by the target sources.
278 Furthermore, ratios to CO are regularly reported in the literature for biomass burning and urban emissions (Baker et
279 al., 2008; Borbon et al., 2013; Brito et al., 2015; Gilman et al., 2015; de Gouw et al., 2017; Koss et al., 2018; Wang
280 et al., 2014) which are useful constraints for further comparisons. Emission ratios were calculated in ppbv of VOC
281 per parts per million by volume (ppmv) of CO, which is similar to a molar ratio (mmol VOC per mol CO). Molar
282 mass (MM) emission ratios were also computed following Gilman et al (2015). MM is the VOC mass emitted (μg
283 m^{-3}) per ppmv CO, obtained from equation 2 and converted by using the VOC molecular weight (MW) (g mol^{-1})
284 and the molar volume (24.86 L at 1 atm and 30 °C). Table S1 includes the emission ratios obtained for each VOC
285 and MW values used.

286

287 2.3.3 VOC-OH reactivity

288 The OH reactivity was estimated to evaluate the potential contribution of each measured VOC to the photochemical
289 processing. VOC-OH reactivity represents the sink reaction of each VOC with the hydroxyl radical (OH) and is equal
290 to

291

$$292 \quad VOC_{OH \text{ reactivity}} = ER \times k_{OH} \times CF, \quad (3)$$

293 where ER is the emission ratio for each VOC related to CO (ppbv per ppmv), k_{OH} is the second-order reaction rate
294 coefficient of VOC with the hydroxyl radical ($\times 10^{-12} \text{ cm}^3 \text{ molec}^{-1} \text{ s}^{-1}$) and CF is the conversion factor of molar
295 concentration ($2.46 \times 10^{10} \text{ molec cm}^{-3} \text{ ppbv}^{-1}$ at 1 atm and 25 °C) (Gilman et al., 2015). k_{OH} values for all VOC
296 species were obtained from Atkinson and Arey (2003a) and the NIST Chemical Kinetics Database (Manion et al.,
297 2015).

298

299 2.3.4 Ozone Formation Potential

300 The oxidation of VOCs is often initiated by the reaction with the hydroxyl radical ($\cdot\text{OH}$), which in the presence of
301 NO_x ($\text{NO} + \text{NO}_2$) leads to the photochemical formation of O_3 . The ozone formation potential represents the ability of
302 each VOC to produce tropospheric ozone and it was calculated as follows:

303

$$304 \quad VOC - \text{ozone formation potential} = ER \times POCP, \quad (4)$$

305 where the ER is the emission ratio of each VOC related to CO (ppbv of VOC per ppmv of CO) and POCP is the
306 photochemical ozone creation potentials developed by Derwent et al. (Derwent et al., 2007, 2010a; Jenkin et al.,
307 2017). POCP values were obtained by simulating a realistic urban mass trajectory with the Master Chemical

308 Mechanism (MCM). This model estimates the change in ozone production by incrementing the mass emission of
309 each VOC (Derwent et al., 1998). POCPs for an individual VOC are estimated by quantifying the effect of a small
310 increase in its emission on the concentration of the formed modelled ozone, respective to that resulting from the same
311 increase in the ethene emission (POCP value for ethene is, therefore, 100). In this study, POCP values were analysed
312 on VOC family basis obtained from a recent study (Huang et al., 2017), or adapted from individual POCP values.

313

314 2.3.5 Secondary organic aerosol (SOA) formation potential

315 The SOA formation potential represents the propensity of each VOC to form secondary organic aerosols and is equal
316 to

$$317 \quad \text{SOA} - \text{VOC formation potential} = ER \times \text{SOAP} , \quad (5)$$

318 where ER is the emission ratio for each measured VOC related to CO (ppbv of VOC per ppmv of CO) and SOAP is
319 a non-dimensional model-derived SOA formation potential (Derwent et al., 2010b; Gilman et al., 2015). All SOAP
320 values represent the modelled mass of organic aerosol that were formed per mass of VOC reacted on an equal mass
321 emitted basis relative to toluene. Toluene was selected as the reference compound due to its well-known emissions
322 and it is usually documented as a critical anthropogenic SOA precursor (Derwent et al., 2010b).

323

324 ER, *k*OH and SOAP values for each VOC and each source are detailed in Table S1. In the absence of SOAP values
325 for specific compounds, we estimated the values (indicated in Table S1, in the 1) by using those of comparable
326 compounds based on similar chemical properties, as suggested in the study of Gilman et al. (2015).

327

328 2.4 Ancillary data

329 Meteorological observations were provided by the NOAA Integrated Surface Database (ISD; [https://](https://www.ncdc.noaa.gov/isd)
330 www.ncdc.noaa.gov/isd for more details). Daily rainfall, air temperature, and wind speed and direction measurements
331 were recorded at the Abidjan Felix Houphouet Boigny Airport. Figure 1 gives the geographical location of the
332 meteorological station and ambient sampling locations.

333

334 3. Results and discussion

335 3.1 Local meteorological conditions

336 Meteorological data from Abidjan, Côte d'Ivoire, are reported in Figure 2. Weekly accumulated precipitation and
337 weekly air temperature means were analysed during 2016, the year of field campaigns. Meteorological conditions in
338 Abidjan are also affected by the monsoon phenomenon which establishes two well defined seasons: a wet season
339 between March and August and a dry season from November to February. The weekly mean air temperature observed
340 was between 24.6 and 29.4 °C, reaching a maximum during the beginning of the wet season (Figure 2). The
341 precipitation pattern shows an increased rate during the monsoon period; however, negative anomalies were observed
342 this year compared with the previous ones (Knippertz et al., 2017). Observed wind patterns during the field campaign
343 showed a predominant contribution from the south-westerly sector with maximum speed during daytime up to 13
344 m.s⁻¹. The high wind speed records reported in Abidjan are higher than those observed in other polluted urban
345 atmospheres (Dominutti et al., 2016; Salameh et al., 2016a; Zhang et al., 2014). The proximity of Abidjan to the
346 ocean and the intrusion of the sea-breeze circulation can facilitate the dispersion processes and, consequently, the

347 urban emissions dilution. Deroubaix et al. (2018) analysed the regional dispersion of urban plumes from SWA coastal
348 cities, i.e. Abidjan, where the inland northward transport of anthropogenic coastal pollutants along with biomass
349 burning emissions were observed.

350

351 3.2 VOCs in Abidjan atmosphere

352 This analysis relies on the fifteen VOC species already listed in Keita et al (2018) and these were measured in both
353 ambient air and at emission sources. These VOCs include 8 aromatics, 3 monoterpenes, 3 alkanes, and isoprene
354 which span a wide range of reactivity and represent the various types of VOC expected to be released by fossil /non-
355 fossil fuel combustion and biogenic emissions.

356

357 3.2.1. Ambient concentrations and spatial distribution

358 The ambient concentration sum of the fifteen quantified VOCs ranged from 6.25 to 72.13 $\mu\text{g m}^{-3}$ (see size-coded pie
359 chart, Figure 3). Higher VOC concentrations were reported in KSI, BIN CRE and PL sites (Figure 3). Details on
360 sampling locations can be found in Table 2. The predominant VOCs are toluene ($4.18 \pm 3.55 \mu\text{g m}^{-3}$), m+p-xylene
361 ($4.05 \pm 3.41 \mu\text{g m}^{-3}$), iso-octane ($2.59 \pm 3.37 \mu\text{g m}^{-3}$), benzene ($1.00 \pm 0.41 \mu\text{g m}^{-3}$), ethylbenzene ($0.93 \pm 0.86 \mu\text{g}$
362 m^{-3}) and limonene ($0.77 \pm 0.76 \mu\text{g m}^{-3}$). Overall, anthropogenic VOCs dominated the ambient profiles by a factor of
363 5 to 20 compared to biogenic ones. BTEX (benzene, toluene, ethylbenzene, and m+p and o-xylenes), a subgroup of
364 aromatic VOCs, usually makes up a significant fraction of the VOC burden in urban atmosphere (Borbon et al., 2018;
365 Boynard et al., 2014; Dominutti et al., 2016). They are emitted by fossil fuel combustion from transport and
366 residential sources as well as evaporation processes such as fuel storage and solvent uses (Borbon et al., 2018). Here
367 their contribution ranged from 35% to 76% of the total VOC burden measured at the ambient sites (Figure 3).
368 Therefore, the following discussion will only focus on BTEX as representative of all measured anthropogenic VOC
369 patterns. Figure 3 shows the spatial distribution of the total VOC concentrations at each site, detailed by the BTEX
370 composition. Firstly, a spatial heterogeneity of the total measured VOC concentration (total values on pie chart,
371 Figure 3) is depicted in the Abidjan district. The spatial variability has been already pointed out by recent studies
372 performed in Abidjan for other atmospheric pollutants (Bahino et al., 2018; Djossou et al., 2018). A spatial
373 heterogeneity was also observed in aerosols concentrations (Djossou et al., 2018), however, maximum aerosols
374 concentrations were reported near domestic fires (KSI, Figure 1) and landfill sites (AD, Figure 1), showing a different
375 pattern than the one observed for the VOC concentrations. Besides of the dilution processes, the spatial distribution
376 of total VOC concentrations seems to be related to the proximity of emission sources, affecting ambient VOC
377 concentrations in the different sampling locations.

378 Second, m+p-xylene and toluene dominate the ambient distribution of BTEX, ranging from 9 to 27 % and 8 to 31 %,
379 respectively. The heterogeneity in VOC spatial distribution could be related to the main activities that are involved
380 in the emission of these compounds. Except for higher benzene contributions observed in some sampling locations
381 such as ABO, AT and FAC, the BTEX profile is rather constant in Abidjan.

382 The mean ambient concentrations observed in Abidjan for alkanes and aromatics were compared with those observed
383 in other cities worldwide (Figure 4). On one hand, mean concentrations in Abidjan depicted lower values when
384 compared with those measured in other cities (blue points in Figure 4). Keita and co-workers (2018) pointed out the
385 high emissions observed in Abidjan sources. In their study, road transport and wood burning VOC emission factors

386 spanned 2 to 100 orders of magnitude, respectively, when compared with those from the literature (Keita et al, 2018).
387 Our ambient observations suggest that wind speed have an important role in the mixing and dilution of the
388 anthropogenic emissions leading to low VOC concentrations in the Abidjan atmosphere.
389 On the other hand, a reasonably good agreement in the relative composition of alkanes and aromatics is observed,
390 showing the same profile in most cities, except for Karachi where higher contributions of heptane and benzene were
391 measured (Barletta et al., 2005). Our results depict that ambient VOC distribution in Abidjan are noticeably similar
392 when compared with northern mid-latitude megacities, suggesting that emissions from fossil fuel combustion for
393 alkanes and aromatics could dominate other regional-specific sources.

394

395 3.2.2. Ambient composition vs. emission source profiles

396 A comparative approach was carried out between ambient and source measurement compositions with the purpose
397 of detecting emission source fingerprints in ambient VOC profiles. Figure 5 reports the relative mass contribution of
398 VOC profiles observed at the nine urban sites together with those obtained from the emission sources. While a
399 noticeable variability in the contribution of emission sources is observed, smoother differences are depicted between
400 the ambient sites. This result reinforces the similar BTEX profiles discussed in the section 3.2.1, where the mixing
401 and dilution process were suggested as the main drivers in the control of ambient emissions. Trimethylbenzenes (124-
402 TMB, 135-TMB, and 123-TMB), mainly observed in road transport emissions, display a dissimilar profile showing
403 higher fractions from sources than ambient sites (Figure 5). These differences might be related to the short lifetime
404 of these compounds (around 4 hours), with a reaction rate ranging from 1.8 to 8.8 ($\times 10^{-15}$ cm³ molecule⁻¹ s⁻¹, (Atkinson
405 and Arey, 2003a)). Their reactivity implies a faster reaction in the atmosphere and losses of these species from the
406 emission to the receptor.

407 On the other hand, in most of the cases, ambient profiles showed higher contributions of alkanes, monoterpenes and
408 isoprene, likely associated with the contribution from different anthropogenic and biogenic sources. The presence of
409 terpenes and isoprene in the profile of all emission sources is notable, mainly in those associated with domestic
410 burning processes, such as charcoal, waste and fuelwood burnings (Figure 5). The terpene emissions from biomass
411 burning were already identified in several studies as they are common species emitted by combustion processes
412 (Gilman et al., 2015; Simpson et al., 2011). Additional studies based on African biomass emissions also reported
413 concentrations of limonene and α -pinene higher than isoprene (Jaars et al., 2016; Saxton et al., 2007).

414 For the selected VOC species, aromatic compounds represent the higher fraction from ambient and source profiles,
415 contributing from 31 to 75% (Figure 5). Comparing the same VOC species in emission sources versus ambient
416 profiles, we found a similarity with the two-wheelers and domestic fires profiles like FW and CH sources.
417 Nevertheless, the VOC ambient profiles obtained from the sites did not show a contrasted difference despite the
418 differences in the activities conducted nearby.

419

420 3.3. Molar mass of measured VOC emissions in Abidjan.

421 Here we compare the composition and magnitude of anthropogenic emissions as a function of molar mass emission
422 ratios as described in section 2.3.2, which is a readily calculated property used to quantify anthropogenic emissions
423 (Gilman et al., 2015). For this analysis, an expanded VOC database of 56 species was considered, including 12
424 terpenes, VOCs of intermediate volatility (IVOCs from C11–C16 n-alkanes), ketones and carbonyl compounds for

425 all sources (Table 1 and Table S1). Species groups were classified according to GEIA groups (Huang et al., 2017)
426 respecting the chemical function of each VOC family (Table S2). In this way, molar masses were also grouped by
427 VOC family from individual values (Table S1). Since the VOCs of intermediate volatility (IVOCs) do not have a
428 specific classification, they were integrated in the group of heavy alkanes (VOC6). Figure 6 shows the contribution
429 of VOC groups to the measured molar mass and the total molar mass of each source, while Figure 7a-d (upper panel)
430 compared the magnitude of measured molar masses for the four leading sectors. As already depicted in the previous
431 section, the distribution reported in Figure 6 reveals the predominance of aromatic molar masses (VOC13-VOC17),
432 ranging from 26 % to 98 %. The prevalence of these compounds is predominantly observed in gasoline-fuelled
433 vehicles, like LDGV and TW sources and diesel light-duty vehicles (LDDV). Alkanes (VOC5+VOC6) also comprise
434 a noticeable molar mass fraction, dominating in TW2T, HDDV and charcoal related sources (by 40, 47 and 53%,
435 respectively).

436 A considerable IVOCs contribution from the emission of HDDV sources was observed, with IVOCs dominating the
437 VOC6 fraction by 30% (considering that VOC6 represents 47% of the total emissions from this source).

438 Interestingly, and as already discussed in section 3.2.2, monoterpenes (VOC11) reported 11%, 13% and 22%
439 contribution in FW, HDDV and WB sources, respectively (Figure 6 and Figure 7b-c). Terpenes in biomass burning
440 sources were already pointed out as the most important compounds together with furans and aromatics in chamber
441 experiments (Koss et al., 2018). Nevertheless, to the extent of our knowledge, their presence in road transport or open
442 waste burning emissions remains unexplored. Regarding OVOCs (VOC22), they were observed in a smaller fraction
443 (less than 7%) apart from HDDV, which contributes to 11% of the total measured molar mass. Previous studies have
444 reported OVOCs as the main fraction in biomass burning emissions (Akagi et al., 2011; Gilman et al., 2015; Yokelson
445 et al., 2013). Moreover, Sekimoto and co-workers also analysed the VOC emission profiles depending on the
446 pyrolysis temperature, showing enrichment of terpenes and non-aromatic oxygenates under high-temperature
447 conditions and an increase in oxygenated aromatics under low-temperature fires (Sekimoto et al., 2018). Comparing
448 the burning-related sources such as FW with previous studies, a lower total measured molar mass was observed in
449 our study than those obtained in the US fuels, by a factor of 33 to 117 (Gilman et al., 2015). In this work, Gilman
450 and co-workers have shown that OVOCs represent 57 to 68% of the total measured molar mass. A different pattern
451 is observed in this study, likely related to the limitation of VOC species measurements by the sampling method
452 deployed, which allows the collection of a limited number of aldehydes (>C6) and other oxygenated compounds as
453 well. Thus, our total molar mass estimation for the sources in Abidjan should be considered as lower limit since
454 additional contributions could be expected from other unknown emitted VOCs, such as OVOCs, alkenes and
455 nitrogenated VOCs.

456 Four sources (TW2T, HDDV, WB, and CH) that represent the leading sectors in the region (road transportation,
457 waste burning, and charcoal emissions) were selected, in order to analyse the magnitude of emissions as a function
458 of molar mass and their potential impacts related to African emissions (next section). Figure 7 (a-d) shows the relative
459 composition and the total molar mass of the measured VOC ($\mu\text{g m}^{-3}$) emitted per ppmv of CO. TW2T sources
460 disclosed the highest molar mass emissions ($4680 \pm 512 \mu\text{g m}^{-3} \text{ ppmv CO}^{-1}$, Figure 7a-d). TW2T emissions were 10
461 to 200 times higher than any other source here analysed, such as heavy-duty vehicles (HDDV, $458 \pm 60 \mu\text{g m}^{-3} \text{ ppmv}$
462 CO^{-1}), wood burning (FW $31.5 \pm 2.50 \mu\text{g m}^{-3} \text{ ppmv CO}^{-1}$), charcoal burning (CH, $43.8 \pm 6.37 \mu\text{g m}^{-3} \text{ ppmv CO}^{-1}$) and
463 light-duty vehicles (LDGV, $137.5 \pm 20 \mu\text{g m}^{-3} \text{ ppmv CO}^{-1}$) emissions (Figure 6).

464 While aromatics (VOC13-VOC17) seem to dominate the molar mass fraction for most sources, their contributions
465 are dissimilar, **dominated** by benzene (VOC13) and toluene (VOC14) in burning-related sources, and by xylenes
466 (VOC15) and trimethylbenzenes (VOC16) in traffic-related ones.

467

468 3.4 Implications on atmospheric reactivity

469 The estimation of the impact on atmospheric chemistry of measured VOC emissions is based in the three metrics
470 described in the section 2.3.

471

472 3.4.1 OH-reactivity of measured VOC emissions

473 Figure 7(e-h) shows the fractional contributions and total VOC-OH reactivity per ppmv of CO for the selected
474 sources. The highest total reactivity is observed from the emissions of TW2T ($488 \pm 43 \text{ s}^{-1} \text{ ppmv CO}^{-1}$), outpacing
475 other sources by a factor of 7 to 170. This disclosed difference is related to the high ERs observed for the more
476 reactive species, like terpenes (VOC11) and C8- and C9-aromatics (VOC15 and VOC16, respectively). Terpenes
477 (VOC11) and aromatics (VOC13-VOC17) altogether are the dominant sink of OH, contributing to 47 to 87% of the
478 total calculated OH reactivity. Individually, terpenes governed the OH-reactivity in open waste burning emissions
479 (76%) and heavy-duty diesel vehicles (60%) (Figure 7f-g). In charcoal burning emissions it may be noted **a singular**
480 fractional contribution of aldehydes (VOC22, 13%) and heavier alkanes (VOC6, 28%), **when compared with other**
481 **sources**. The modest presence of alkenes in the VOC-OH fractional analysis, well-known for their high reactivity
482 effects, is related to the limitation of the sampling method which **does not allow** the collection of light alkene species.
483 We might expect a high contribution of alkenes adding to the terpene burden.

484

485 3.4.2 Ozone formation potential of measured VOC emissions

486 Overall, the fractional ozone formation distribution is dominated by aromatics (VOC13 to VOC17) in all sources, by
487 38 to 63%. Alkanes (VOC6) represent a significant contribution in charcoal burning, HDDV, and TW2T, accounting
488 for 45, 28 and 26%, respectively. It is important to note the terpenes (VOC11) contribution, coming not only from
489 burning sources but also from the road transportation sector (Figure 7i-l). Aldehydes (VOC22) are well-known due
490 to their high reactivity in the atmosphere (Atkinson and Arey, 2003a; Sommariva et al., 2011), and some of these
491 species have shown a large impact on ozone formation and chemistry. In our estimation, we can observe the
492 contribution of these compounds mainly from diesel (HDDV) and charcoal burning sources (CH). The total potential
493 ozone was computed for each source, showing most of the time a dominant contribution from TW2T (80343 POCP
494 ppmv CO^{-1}), which is 13, 24 and 150 times higher than the potential impact in ozone formation derived from HDDV,
495 WB and CH emissions, respectively.

496

497 3.4.3 SOA formation potential of measured VOC emissions

498 Figure 7 (m-p) shows the composition and mean SOA formation potentials of VOC families emitted by each selected
499 source. As can be expected, charcoal burning reports the lowest SOAP (335 SOAP per ppmv CO^{-1}), compared with
500 TW2T, HDDV and WB sources, whose SOAPs values are 147, 10 and 9 times greater, respectively. Globally,
501 aromatics (VOC13-VOC17) governed the SOA formation in our estimations, by 72 to 98%. Interestingly, terpenes
502 (VOC11) represented a minor contribution in the SOA formation, presenting a SOAP index lower than for aromatic

503 species. It represents approximately 20% of the SOAP for toluene (VOC14). Despite the well-known role of terpenes
504 as SOA precursors (Ait-Helal et al., 2014), the method used here is not able to correctly quantify their contributions
505 to SOA formation. The differences between SOAP values and measured aerosols yield were already pointed out by
506 Gilman and co-authors (Gilman et al., 2015), who performed some sensitivity tests in order to harmonize SOAP and
507 aerosols yields. We performed the same analysis here, adjusting the SOAP terpene values to be 10% higher. The
508 results in total SOAP per ppmv of CO did not show considerable increases in any of the sources, expanding the total
509 SOAP up to 1%. Similar results were observed for fractional distribution, so that the changes in terpenes SOAPs
510 (VOC11) did not show any substantial change in the VOC contribution for SOA formation. These findings are in
511 agreement with those identified in the study of Gilman et al. (2015), suggesting an underestimation in the fractional
512 contribution of terpenes to the potential formation of organic aerosols over SWA region.

513

514 3.5 *Quantification of VOC emissions*

515 Anthropogenic VOC emissions were quantified by considering the complete VOC dataset, which includes the 56
516 compounds analysed, aldehydes, IVOCs and terpenes species. Mean residential emissions are also integrated and
517 compared with those from the EDGAR v4.3.2 inventory. Additionally, we incorporate the residential and road
518 transport profiles provided by the MACCity inventory (Granier et al., 2011), available in the ECCAD-GEIA database
519 (<http://eccad.aeris-data.fr>). The main differences between both global inventories are related to the speciation level
520 of VOCs families. MACCity considers all the aromatics in the same VOC group; thus, we provide here the sum of
521 VOC13 to VOC17 families (Table S2) to compare it with the aromatics group from our quantification.

522 Figure 8 exhibits the speciated emissions calculated for Côte d'Ivoire along with those provided by the two emission
523 inventories. Globally, the discrepancies already highlighted in the previous analysis are exacerbated by introducing
524 the complete VOC database. Calculated residential emissions are greater by a factor of 14 and 43 when compared
525 with EDGAR v4.3.2 and MACCity, respectively (Figure 8a). In terms of composition, the main differences observed
526 are related to the VOC22 group (aldehydes). This group discloses a higher contribution by a factor of 5 in the EDGAR
527 inventory, accounting for 64% of the total emission. There is also a disparity in the contribution from aromatics (sum
528 of VOC13 to VOC17) and alkenes (VOC12), which reveals a more substantial influence in the MACCity profile
529 (58% and 22%, respectively) (Figure 8a). This disparity could be related to the few VOC species that were analysed
530 for the VOC12 group in our study. Nevertheless, aromatics dominate the fractional contribution in our calculated
531 emissions (39%), especially toluene (VOC14) and C8-aromatics (VOC15) (11% and 10%, respectively). Alkanes
532 (>VOC6 alkanes) show a more significant contribution in the residential profile, in which IVOCs contribute 20% of
533 the total calculated alkanes obtained by our estimations.

534 Regarding the road transportation sector, total calculated emissions are higher than the global inventories by a factor
535 of 100 and 160 for EDGAR and MACCity, respectively (Figure 8a). A moderate agreement is observed with
536 speciation (Figure 8b). Aromatics and alkanes are the main contributions for all profiles in different proportions. Our
537 estimates report the most significant contributions in C8-aromatics (VOC15), C9-aromatics (VOC16) and toluene
538 (VOC14), with a 25, 14 and 10% contribution, respectively (Figure 8c and Figure 9). In comparison, EDGAR v4.3.2
539 shows a contribution of 9% for VOC15, 3.5% for VOC16 and 13% for VOC14 (Figure 9). Road transport profiles
540 also reproduce the anomalies in the VOC12 (alkenes) contribution observed in the residential sector, presenting

541 greater emissions in the global inventories. The comparison between both inventories also depicted considerable
542 discrepancies, of a factor of 3.

543 A similar profile is observed for heavier alkanes (VOC6) which present an analogous contribution between our
544 estimation and EDGAR emissions (34 and 37%, respectively; Figure 8b). Nevertheless, the alkanes (VOC5+VOC6)
545 contribution in the MACCity profiles prevails over road transport emissions accounting for 62%.

546 Interestingly, terpenes and isoprene emissions can be denoted in both sectors in the Côte d'Ivoire calculated emissions
547 (VOC11 and VOC10). Despite the reduced contribution of these species (9% in residential and 4% in road transport),
548 the underestimation of them in the emissions from anthropogenic sources could have consequences for the
549 atmospheric chemistry. Since the reactivity is specific for each VOC, the inaccuracies in the speciation could also
550 have implications on the estimation of their impacts. Specifically for terpenes (VOC11), it can be noted that their
551 contribution in the *k*OH reactivity, accounting for 42% in the residential sector and 28% in road transport reactivity
552 (Figure 8c). Even though the total OH reactivity in all profiles is rather similar, the alkenes fraction in this study is
553 not well-represented which could increase the contribution in terms of reactivity.

554 Figure 9 also displays the residential and road transportation profiles obtained from Côte d'Ivoire, compared with
555 EDGAR v4.3.2 profiles for Europe. Noticeably in our estimations, road transport and residential sectors presented
556 comparable total emissions, whereas those from the EDGAR inventory were different by a factor of 8 (86.1 vs 12.1
557 Gg year⁻¹, respectively). Similar disagreements are also observed when comparing EDGAR total emissions for
558 Europe with Côte d'Ivoire, where the former presents larger emissions (198 vs 86 and 433 vs 12 Gg year⁻¹,
559 respectively). We highlight here the substantial differences in total emissions, outpacing those estimated for Europe
560 by a factor of 3 for road transport and by a factor of 6 for residential sector (433 and 198 Gg year⁻¹, respectively).

561 The lack of measurements and source profile data in Africa was previously pointed out in the development of EDGAR
562 inventory, which led to considering the priority of this region for future inventory improvements (Huang et al., 2017).
563 Even though our VOC database is not extensive for all the species emitted by the sources analysed, the incorporation
564 of new VOC species reinforces the usefulness of *in situ* measurements under real conditions to derive realistic
565 emission factors and subsequent estimates of representative emission profiles.

566

567 3.6 Anthropogenic emissions of terpenes, IVOCs and aldehydes in SWA

568 As previously highlighted, terpenes commonly emitted by biogenic sources were observed in the emissions from
569 anthropogenic sources. Global emission inventories wholly neglect these emissions; however, they could have
570 considerable effects in the atmospheric chemical processing, by producing secondary pollutants in the atmosphere.
571 Figure 10a reports the fractional distribution of terpenes in several analysed emission sources. The main contributions
572 are associated with the emissions from waste burning (WB, 47%), two-wheel vehicles (TW2T, 20%), wood burning
573 (FW, 17%) and charcoal making (CHM, 14%) sources. The total annual emissions estimated for these compounds,
574 which represents 334 Gg year⁻¹ and 11% of the total emissions, cannot be neglected when compared with the emission
575 of other well-known anthropogenic VOC, i.e. C9-aromatics. Evaluating the distribution by terpenes species among
576 the emission sources permits a different pattern to be noted (Figure 11). While terpenes emissions from road transport
577 are mainly dominated by α -ocimene and α -terpinolene, limonene and isoprene are controlled by wood-burning
578 sources. The main wood types burnt in Côte d'Ivoire are Hevea (*Hevea brasiliensis*) and Iroko (*Milicia excelsa*),
579 which are widely used in urban domestic fires for cooking, heating and other services (Keita et al., 2018). In our

580 study, we only present the results obtained from Hevea, a tropical African hardwood, characterised as a species that
581 emits monoterpenes (Bracho-Nunez et al., 2013; Wang et al., 2007). The principal monoterpene compounds naturally
582 emitted by Hevea species are sabinene, limonene, and α -pinene (Bracho-Nunez et al., 2013). The isoprene emissions
583 from non-isoprene emitting species were already observed in biomass burning studies, which indicates that isoprene
584 is formed during the combustion process (Hatch et al., 2015).

585 As it can be noted in Figure 11, isoprene emissions are also impacted by vehicles, mainly TW sources, and camphene
586 and β -pinene emissions by HDDV sources. The anthropogenic sources of isoprene have been documented in urban
587 areas, mainly associated with traffic emissions (Borbon et al., 2001; von Schneidemesser et al., 2011). However, to
588 the best of our knowledge, no previous studies have ever analysed the presence of monoterpenes from road
589 transportation sources. α -pinene and β -pinene emissions are ruled by charcoal burning fires, which also contribute in
590 some fraction to the emissions of isoprene and limonene. In contrast, charcoal making emissions are dominated by
591 γ -terpinene and isoprene. The results from biomass burning sources provided here were obtained from non-controlled
592 experiments, which did not allow the evaluation of differences between the emissions from each combustion phase
593 (pyrolysis, flaming and smouldering). Further investigation is needed in order to develop a better understanding of
594 these differences and to characterize the different combustion phases.

595 VOCs of intermediate volatility are suspected to be efficient precursors of SOA (Seinfeld and Pandis, 2006 and
596 references therein). However, as it was discussed in the section 3.4.3, our method was not able to resolve the
597 differences between VOC families and most SOAP was assigned to aromatic compounds (up to 98%). Figure 11b
598 reports the fractional contribution and total emissions of IVOCs. CHM, FW, HDDV, and TW represent the primary
599 sources of these compounds, accounting for 58, 15, 12 and 11% of the total, respectively. Despite their lower
600 emissions compared with aromatics or terpenes, IVOCs are estimated to account for 80 Gg year⁻¹ of emissions in
601 Côte d'Ivoire. A recent study observed that fine particles in Abidjan are three times higher than the World Health
602 Organisation recommended concentrations (Djossou et al., 2018). Hence, a better understanding of the aerosol
603 precursors and formation processes is essential for the later reduction of their concentrations in the urban atmosphere.
604 Oxygenated compounds were previously indicated as essential species in the emissions from burning sources
605 (Gilman et al., 2015; Hatch et al., 2015; Koss et al., 2018; Wiedinmyer et al., 2014). In addition, oxygenated
606 compounds like non-aromatics were dominant in the burning emission sources including a range of functional groups,
607 of which alcohols and carbonyls were the most abundant (Koss et al., 2018; Stockwell et al., 2015). Figure 11c
608 shows that aldehyde emissions are mainly governed by charcoal fabrication (CHM), two-wheel vehicles (TW) and
609 wood burning sources (Figure 11c). In our study the quantified aldehydes represent only 5.5% of the total emissions
610 of the country (170 Gg year⁻¹). However, they can be essential compounds concerning reactivity and ozone formation.
611 Hence, further analysis of oxygenated compounds together with furans and other nitro-oxygenated compounds needs
612 to be addressed in future campaigns, in order to improve not only the quantification of these compounds but also
613 provide a better identification of the African tracers from biomass burning processes.

614

615 4. Summary and conclusions

616 This study reports for the first time a chemically detailed range of VOCs including C5-C16 alkanes, monoterpenes,
617 alkenes, aromatics and carbonyls compounds by using sorbent tubes during an intensive field campaign in Abidjan,
618 SWA. We present here an original dataset integrating main emission sources and ambient measurements from nine

619 representative sites, and covering the urban spatial distribution of VOCs in Abidjan. The spatial distribution and
620 composition of VOC in ambient air in Abidjan reveals the effect of biomass burning and traffic emissions. The
621 highest concentrations were observed near domestic fires, landfill fires and traffic sites, in agreement with the results
622 reported in previous studies, when gas-phase and aerosols pollutants were measured (Bahino et al., 2018; Djossou et
623 al., 2018).

624 The calculation of emission ratios is an important metric to evaluate the estimates provided by global emission
625 inventories. Emission ratios from regional-specific emission sources were established here and later used for the
626 analysis of fractional molar mass contribution and the estimation of potential VOC-OH reactivity, ozone and
627 secondary organic aerosol formation. The distribution of VOC emissions (magnitude and composition) was different
628 for each evaluated source. Two wheel and heavy-duty vehicle sources presented the most significant total molar mass
629 emissions, while charcoal-burning was the lowest. The sources related to burning processes, such as waste and wood
630 burning, also presented significant contribution to VOCs emissions. These sources represent common activities
631 present in Abidjan and might contribute a large quantity of VOC emissions to the SWA region.

632 Regarding VOC speciation, molar mass contributions were mostly dominated by aromatic and alkane compounds.
633 Since few alkene species were identified, aromatics ruled both ozone and SOA formation potential. However, the
634 SOA metrics applied here were not able to accurately analyse the other important SOA precursors contribution, such
635 as monoterpenes. Nevertheless, monoterpenes can contribute significantly to VOC-OH reactivity from some sources
636 like WB, and the alkanes species can significantly contribute to the total reactivity.

637 In order to estimate the magnitude of VOC emissions in Côte d'Ivoire, emission factors were determined from the
638 *in-situ* VOC database. Road transportation and residential profiles were obtained and compared with those reported
639 in global emission inventories (MACCcity and EDGAR). Our results revealed a discrepancy of up to a factor of 43
640 and 160 for residential and transport profiles when compared with both referenced inventories. The high levels of
641 VOC emissions obtained for Côte d'Ivoire outpace European emissions by up to a factor of 6. Interestingly,
642 monoterpene emissions were observed in anthropogenic emission sources from biomass burning to road
643 transportation sources, contributing to up to 340 Gg year⁻¹ to the annual emissions. These compounds are generally
644 missing in the global anthropogenic emission profiles, which would underestimate their impacts on air quality. This
645 underestimation is not only expected for Côte d'Ivoire but for all West Africa countries.

646 This study, in the framework of the DACCIWA project, allowed us for the first time to identify and quantify several
647 VOCs in ambient air and at emission sources in Abidjan, Côte d'Ivoire. Our results provide significant constraints
648 for the development of more realistic regional emission inventories. A continuous effort is needed to collect new
649 emission data and ambient measurements in West African countries for all critical atmospheric pollutants.

650

651 **Acknowledgments**

652 This work has received funding from the European Union Seventh Framework Programme (FP7/2007-2013) under
653 grant agreement number 603502 (EU project DACCIWA: Dynamics-aerosol-chemistry-cloud interactions in West
654 Africa). P Dominutti acknowledges the Postdoctoral Fellowship support from the Université Clermont Auvergne and
655 thanks the grant received from the CAPES program (Process N°: 88887.098995/2015-00, CAPES – PVE's Program,
656 2014) from the Ministry of Education of Brazil, during 2015-2016. Thierry Leonardis is thanked for the contribution
657 in the analysis of VOC sorbent tubes, graciously performed at the SAGE Department at IMT Lille Douai (France).

658

659 *Data availability.*

660 All data used in this study will be publicly available soon on the AERIS Data and Service Center, which can
661 be found at <http://baobab.sedoo.fr/DACCIWA>.

662

663 *Competing interests.* The authors declare that they have no conflict of interest.

664

666 **References**

- 667 AIRPARIF: Surveillance de la qualité de l'air en Ile-de-France., [online] Available from:
668 <http://www.airparif.asso.fr/> (Accessed 1 March 2018), 2013.
- 669 Ait-Helal, W., Borbon, A., Sauvage, S., De Gouw, J. A., Colomb, A., Gros, V., Freutel, F., Crippa, M., Afif, C.,
670 Baltensperger, U., Beekmann, M., Doussin, J. F., Durand-Jolibois, R., Fronval, I., Grand, N., Leonardis, T.,
671 Lopez, M., Michoud, V., Miet, K., Perrier, S., Prévôt, A. S. H., Schneider, J., Siour, G., Zapf, P. and Locoge, N.:
672 Volatile and intermediate volatility organic compounds in suburban Paris: Variability, origin and importance for
673 SOA formation, *Atmos. Chem. Phys.*, 14(19), 10439–10464, doi:10.5194/acp-14-10439-2014, 2014.
- 674 Ait-Helal, W., Beeldens, A., Boonen, E., Borbon, A., Boréave, A., Cazaunau, M., Chen, H., Daële, V., Dupart,
675 Y., Gaimoz, C., Gallus, M., George, C., Grand, N., Grosselin, B., Herrmann, H., Ifang, S., Kurtenbach, R., Maille,
676 M., Marjanovic, I., Mellouki, A., Miet, K., Mothes, F., Poulain, L., Rabe, R., Zapf, P., Kleffmann, J. and Doussin,
677 J.-F.: On-road measurements of NMVOCs and NO_x: Determination of light-duty vehicles emission factors from
678 tunnel studies in Brussels city center, *Atmos. Environ.*, 122, 799–807, doi:10.1016/j.atmosenv.2015.09.066, 2015.
- 679 Akagi, S. K., Yokelson, R. J., Wiedinmyer, C., Alvarado, M. J., Reid, J. S., Karl, T., Crounse, J. D. and Wennberg,
680 P. O.: Emission factors for open and domestic biomass burning for use in atmospheric models, *Atmos. Chem.*
681 *Phys.*, 11(9), 4039–4072, doi:10.5194/acp-11-4039-2011, 2011.
- 682 Assamoi, E.-M. and Lioussé, C.: A new inventory for two-wheel vehicle emissions in West Africa for 2002,
683 *Atmos. Environ.*, 44(32), 3985–3996, doi:10.1016/j.atmosenv.2010.06.048, 2010.
- 684 Atkinson, R. and Arey, J.: Atmospheric Degradation of Volatile Organic Compounds, *Chem. Rev.*, 103(12),
685 4605–4638, doi:10.1021/cr0206420, 2003a.
- 686 Atkinson, R. and Arey, J.: Gas-phase tropospheric chemistry of biogenic volatile organic compounds: a review,
687 *Atmos. Environ.*, 37(2), 197–219, doi:10.1016/S1352-2310(03)00391-1, 2003b.
- 688 Bahino, J., Yoboué, V., Galy-Lacaux, C., Adon, M., Akpo, A., Keita, S., Lioussé, C., Gardrat, E., Chiron, C.,
689 Ossouhou, M., Gnamien, S. and Djossou, J.: A pilot study of gaseous pollutants' measurement (NO₂, SO₂, NH₃,
690 HNO₃ and O₃) in Abidjan, Côte d'Ivoire: contribution to an overview of gaseous pollution in African cities,
691 *Atmos. Chem. Phys.*, 18(7), 5173–5198, doi:10.5194/acp-18-5173-2018, 2018.
- 692 Baker, A. K., Beyersdorf, A. J., Doezema, L. a., Katzenstein, A., Meinardi, S., Simpson, I. J., Blake, D. R. and
693 Sherwood, F. R.: Measurements of nonmethane hydrocarbons in 28 United States cities, *Atmos. Environ.*, 42(1),
694 170–182, doi:10.1016/j.atmosenv.2007.09.007, 2008.
- 695 Barletta, B., Meinardi, S., Simpson, I. J., Khwaja, H. a, Blake, D. R. and Rowland, F. S.: Mixing ratios of volatile
696 organic compounds (VOCs) in the atmosphere of Karachi, Pakistan, *Atmos. Environ.*, 36(21), 3429–3443,
697 doi:10.1016/S1352-2310(02)00302-3, 2002.
- 698 Barletta, B., Meinardi, S., Sherwood, F. R., Chan, C.-Y., Wang, X., Zou, S., Yin Chan, L. and Blake, D. R.:
699 Volatile organic compounds in 43 Chinese cities, *Atmos. Environ.*, 39(32), 5979–5990,
700 doi:10.1016/j.atmosenv.2005.06.029, 2005.

701 Bechara, J., Borbon, A., Jambert, C., Colomb, A. and Perros, P. E.: Evidence of the impact of deep convection on
702 reactive Volatile Organic Compounds in the upper tropical troposphere during the AMMA experiment in West
703 Africa, *Atmos. Chem. Phys.*, 10(21), 10321–10334, doi:10.5194/acp-10-10321-2010, 2010.

704 Bon, D. M., Ulbrich, I. M., de Gouw, J. a., Warneke, C., Kuster, W. C., Alexander, M. L., Baker, A., Beyersdorf,
705 a. J., Blake, D., Fall, R., Jimenez, J. L., Herndon, S. C., Huey, L. G., Knighton, W. B., Ortega, J., Springston, S.
706 and Vargas, O.: Measurements of volatile organic compounds at a suburban ground site (T1) in Mexico City
707 during the MILAGRO 2006 campaign: measurement comparison, emission ratios, and source attribution, *Atmos.*
708 *Chem. Phys.*, 11(6), 2399–2421, doi:10.5194/acp-11-2399-2011, 2011.

709 Borbon, A., Fontaine, H., Veillerot, M., Locoge, N., Galloo, J. C. and Guillermo, R.: An investigation into the
710 traffic-related fraction of isoprene at an urban location, *Atmos. Environ.*, 35(22), 3749–3760, doi:10.1016/S1352-
711 2310(01)00170-4, 2001.

712 Borbon, A., Gilman, J. B., Kuster, W. C., Grand, N., Chevaillier, S., Colomb, A., Dolgorouky, C., Gros, V., Lopez,
713 M., Sarda-Esteve, R., Holloway, J., Stutz, J., Petetin, H., McKeen, S., Beekmann, M., Warneke, C., Parrish, D.
714 D. and de Gouw, J. A.: Emission ratios of anthropogenic volatile organic compounds in northern mid-latitude
715 megacities: Observations versus emission inventories in Los Angeles and Paris, *J. Geophys. Res. Atmos.*, 118(4),
716 2041–2057, doi:10.1002/jgrd.50059, 2013.

717 Borbon, A., Boynard, A., Salameh, T., Baudic, A., Gros, V., Gauduin, J., Perrussel, O. and Pallares, C.: Is Traffic
718 Still an Important Emitter of Monoaromatic Organic Compounds in European Urban Areas?, *Environ. Sci.*
719 *Technol.*, 52(2), 513–521, doi:10.1021/acs.est.7b01408, 2018.

720 Boynard, A., Borbon, A., Leonardis, T., Barletta, B., Meinardi, S., Blake, D. R. and Locoge, N.: Spatial and
721 seasonal variability of measured anthropogenic non-methane hydrocarbons in urban atmospheres: Implication on
722 emission ratios, *Atmos. Environ.*, 82, 258–267, doi:10.1016/j.atmosenv.2013.09.039, 2014.

723 Bracho-Nunez, A., Knothe, N. M., Welter, S., Staudt, M., Costa, W. R., Liberato, M. A. R., Piedade, M. T. F. and
724 Kesselmeier, J.: Leaf level emissions of volatile organic compounds (VOC) from some Amazonian and
725 Mediterranean plants, *Biogeosciences*, 10(9), 5855–5873, doi:10.5194/bg-10-5855-2013, 2013.

726 Brito, J., Wurm, F., Yáñez-Serrano, A. M., de Assunção, J. V., Godoy, J. M. and Artaxo, P.: Vehicular Emission
727 Ratios of VOCs in a Megacity Impacted by Extensive Ethanol Use: Results of Ambient Measurements in São
728 Paulo, Brazil, *Environ. Sci. Technol.*, 49(19), 11381–11387, doi:10.1021/acs.est.5b03281, 2015.

729 Deroubaix, A., Menut, L., Flamant, C., Brito, J., Denjean, C., Dreiling, V., Fink, A., Jambert, C., Kalthoff, N.,
730 Knippertz, P., Ladkin, R., Mailler, S., Maranan, M., Pacifico, F., Piguet, B., Siour, G. and Turquety, S.: Diurnal
731 cycle of coastal anthropogenic pollutant transport over southern West Africa during the DACCIWA campaign,
732 *Atmos. Chem. Phys. Discuss.*, (August), 1–44, doi:10.5194/acp-2018-766, 2018.

733 Derwent, R. G., Jenkin, M. E., Saunders, S. M. and Pilling, M. J.: Photochemical ozone creation potentials for
734 organic compounds in northwest Europe calculated with a master chemical mechanism, *Atmos. Environ.*, 32(14–
735 15), 2429–2441, doi:10.1016/S1352-2310(98)00053-3, 1998.

736 Derwent, R. G., Jenkin, M. E., Passant, N. R. and Pilling, M. J.: Reactivity-based strategies for photochemical

737 ozone control in Europe, *Environ. Sci. Policy*, 10(5), 445–453, doi:10.1016/j.envsci.2007.01.005, 2007.

738 Derwent, R. G., Jenkin, M. E., Pilling, M. J., Carter, W. P. L. and Kaduwela, A.: Reactivity scales as comparative
739 tools for chemical mechanisms., *J. Air Waste Manag. Assoc.*, 60(8), 914–924, doi:10.3155/1047-3289.60.8.914,
740 2010a.

741 Derwent, R. G., Jenkin, M. E., Utembe, S. R., Shallcross, D. E., Murrells, T. P. and Passant, N. R.: Secondary
742 organic aerosol formation from a large number of reactive man-made organic compounds, *Sci. Total Environ.*,
743 408(16), 3374–3381, doi:10.1016/j.scitotenv.2010.04.013, 2010b.

744 Detournay, A., Sauvage, S., Locoge, N., Gaudion, V., Leonardis, T., Fronval, I., Kaluzny, P. and Galloo, J.-C.:
745 Development of a sampling method for the simultaneous monitoring of straight-chain alkanes, straight-chain
746 saturated carbonyl compounds and monoterpenes in remote areas., *J. Environ. Monit.*, 13(4), 983–90,
747 doi:10.1039/c0em00354a, 2011.

748 Djossou, J., Léon, J.-F., Akpo, A. B., Lioussé, C., Yoboué, V., Bedou, M., Bodjrenou, M., Chiron, C., Galy-
749 Lacaux, C., Gardrat, E., Abbey, M., Keita, S., Bahino, J., N'Datchoh, E. T., Ossohou, M. and Awanou, C. N.:
750 Mass concentration, optical depth and carbon composition of particulate matter in the major southern West
751 African cities of Cotonou (Benin) and Abidjan (Côte d'Ivoire), *Atmos. Chem. Phys.*, 18(9), 6275–6291,
752 doi:10.5194/acp-18-6275-2018, 2018.

753 Dominutti, P. A., Nogueira, T., Borbon, A., Andrade, M. de F. and Fornaro, A.: One-year of NMHCs hourly
754 observations in São Paulo megacity: meteorological and traffic emissions effects in a large ethanol burning
755 context, *Atmos. Environ.*, 142, 371–382, doi:10.1016/j.atmosenv.2016.08.008, 2016.

756 Gaimoz, C., Sauvage, S., Gros, V., Herrmann, F., Williams, J., Locoge, N., Perrussel, O., Bonsang, B.,
757 D'Argouges, O., Sarda-Estève, R. and Sciare, J.: Volatile organic compounds sources in Paris in spring 2007. Part
758 II: source apportionment using positive matrix factorisation, *Environ. Chem.*, 8(1), 91, doi:10.1071/EN10067,
759 2011.

760 Gilman, J. B., Lerner, B. M., Kuster, W. C., Goldan, P. D., Warneke, C., Veres, P. R., Roberts, J. M., De Gouw,
761 J. A., Burling, I. R. and Yokelson, R. J.: Biomass burning emissions and potential air quality impacts of volatile
762 organic compounds and other trace gases from fuels common in the US, *Atmos. Chem. Phys.*, 15(24), 13915–
763 13938, doi:10.5194/acp-15-13915-2015, 2015.

764 de Gouw, J. A., Gilman, J. B., Kim, S. W., Lerner, B. M., Isaacman-VanWertz, G., McDonald, B. C., Warneke,
765 C., Kuster, W. C., Lefer, B. L., Griffith, S. M., Dusanter, S., Stevens, P. S. and Stutz, J.: Chemistry of Volatile
766 Organic Compounds in the Los Angeles basin: Nighttime Removal of Alkenes and Determination of Emission
767 Ratios, *J. Geophys. Res. Atmos.*, 122(21), 11,843-11,861, doi:10.1002/2017JD027459, 2017.

768 Granier, C., Bessagnet, B., Bond, T., D'Angiola, A., Denier van der Gon, H., Frost, G. J., Heil, A., Kaiser, J. W.,
769 Kinne, S., Klimont, Z., Kloster, S., Lamarque, J.-F., Lioussé, C., Masui, T., Meleux, F., Mieville, A., Ohara, T.,
770 Raut, J.-C., Riahi, K., Schultz, M. G., Smith, S. J., Thompson, A., van Aardenne, J., van der Werf, G. R. and van
771 Vuuren, D. P.: Evolution of anthropogenic and biomass burning emissions of air pollutants at global and regional
772 scales during the 1980–2010 period, *Clim. Change*, 109(1–2), 163–190, doi:10.1007/s10584-011-0154-1, 2011.

773 Hatch, L. E., Luo, W., Pankow, J. F., Yokelson, R. J., Stockwell, C. E. and Barsanti, K. C.: Identification and
774 quantification of gaseous organic compounds emitted from biomass burning using two-dimensional gas
775 chromatography-time-of-flight mass spectrometry, *Atmos. Chem. Phys.*, 15(4), 1865–1899, doi:10.5194/acp-15-
776 1865-2015, 2015.

777 Huang, G., Brook, R., Crippa, M., Janssens-Maenhout, G., Schieberle, C., Dore, C., Guizzardi, D., Muntean, M.,
778 Schaaf, E. and Friedrich, R.: Speciation of anthropogenic emissions of non-methane volatile organic compounds:
779 A global gridded data set for 1970-2012, *Atmos. Chem. Phys.*, 17(12), 7683–7701, doi:10.5194/acp-17-7683-
780 2017, 2017.

781 Jaars, K., Beukes, J. P., Van Zyl, P. G., Venter, A. D., Josipovic, M., Pienaar, J. J., Vakkari, V., Aaltonen, H.,
782 Laakso, H., Kulmala, M., Tiitta, P., Guenther, A., Hellén, H., Laakso, L. and Hakola, H.: Ambient aromatic
783 hydrocarbon measurements at Welgegund, South Africa, *Atmos. Chem. Phys.*, 14(13), 7075–7089,
784 doi:10.5194/acp-14-7075-2014, 2014.

785 Jaars, K., Van Zyl, P. G., Beukes, J. P., Hellén, H., Vakkari, V., Josipovic, M., Venter, A. D., Räsänen, M.,
786 Knoetze, L., Cilliers, D. P., Siebert, S. J., Kulmala, M., Rinne, J., Guenther, A., Laakso, L. and Hakola, H.:
787 Measurements of biogenic volatile organic compounds at a grazed savannah grassland agricultural landscape in
788 South Africa, *Atmos. Chem. Phys.*, 16(24), 15665–15688, doi:10.5194/acp-16-15665-2016, 2016.

789 Jenkin, M. E., Derwent, R. G. and Wallington, T. J.: Photochemical ozone creation potentials for volatile organic
790 compounds: Rationalization and estimation, *Atmos. Environ.*, 163(x), 128–137,
791 doi:10.1016/j.atmosenv.2017.05.024, 2017.

792 Keita, S., Lioussé, C., Yoboué, V., Dominutti, P., Guinot, B., Assamoi, E.-M., Borbon, A., Haslett, S. L., Bouvier,
793 L., Colomb, A., Coe, H., Akpo, A., Adon, J., Bahino, J., Doumbia, M., Djossou, J., Galy-Lacaux, C., Gardrat, E.,
794 Gnamien, S., Léon, J. F., Ossouhou, M., N’Datchoh, E. T. and Roblou, L.: Particle and VOC emission factor
795 measurements for anthropogenic sources in West Africa, *Atmos. Chem. Phys.*, 18(10), 7691–7708,
796 doi:10.5194/acp-18-7691-2018, 2018.

797 Knippertz, P., Evans, M. J., Field, P. R., Fink, A. H., Lioussé, C. and Marsham, J. H.: The possible role of local
798 air pollution in climate change in West Africa, *Nat. Clim. Chang.*, 5(9), 815–822, doi:10.1038/nclimate2727,
799 2015.

800 Knippertz, P., Fink, A. H., Deroubaix, A., Morris, E., Tocquer, F., Evans, M. J., Flamant, C., Gaetani, M.,
801 Lavaysse, C., Mari, C., Marsham, J. H., Meynadier, R., Affo-Dogo, A., Bahaga, T., Brosse, F., Deetz, K., Guebsi,
802 R., Latifou, I., Maranan, M., Rosenberg, P. D. and Schlueter, A.: A meteorological and chemical overview of the
803 DACCIWA field campaign in West Africa in June-July 2016, *Atmos. Chem. Phys.*, 17(17), 10893–10918,
804 doi:10.5194/acp-17-10893-2017, 2017.

805 Koss, A. R., Sekimoto, K., Gilman, J. B., Selimovic, V., Coggon, M. M., Zarzana, K. J., Yuan, B., Lerner, B. M.,
806 Brown, S. S., Jimenez, J. L., Krechmer, J., Roberts, J. M., Warneke, C., Yokelson, R. J. and De Gouw, J.: Non-
807 methane organic gas emissions from biomass burning: Identification, quantification, and emission factors from
808 PTR-ToF during the FIREX 2016 laboratory experiment, *Atmos. Chem. Phys.*, 18(5), 3299–3319,
809 doi:10.5194/acp-18-3299-2018, 2018.

810 Kumar, A., Singh, D., Kumar, K., Singh, B. B. and Jain, V. K.: Distribution of VOCs in urban and rural
811 atmospheres of subtropical India: Temporal variation, source attribution, ratios, OFP and risk assessment, *Sci.*
812 *Total Environ.*, 613–614, 492–501, doi:10.1016/j.scitotenv.2017.09.096, 2018.

813 Liousse, C., Assamoi, E., Criqui, P., Granier, C. and Rosset, R.: Explosive growth in African combustion
814 emissions from 2005 to 2030, *Environ. Res. Lett.*, 9(3), 035003, doi:10.1088/1748-9326/9/3/035003, 2014.

815 Manion, J. A., Huie, R. E., Levin, R. D., Jr., D. R. B., Orkin, V. L., Tsang, W., McGivern, W. S., Hudgens, J. W.,
816 Knyazev, V. D., Atkinson, D. B., Chai, E., Tereza, A. M., Lin, C.-Y., Allison, T. C., Mallard, W. G., Westley, F.,
817 Herron, J. T., R. F. Hampson, A. and Frizzell, D. H.: NIST Chemical Kinetics Database, Gaithersburg, Maryland.
818 [online] Available from: <http://kinetics.nist.gov/> (Accessed 18 April 2018), 2015.

819 Mari, C. H., Reeves, C. E., Law, K. S., Ancellet, G., Andrés-Hernández, M. D., Barret, B., Bechara, J., Borbon,
820 A., Bouarar, I., Cairo, F., Commane, R., Delon, C., Evans, M. J., Fierli, F., Floquet, C., Galy-Lacaux, C., Heard,
821 D. E., Homan, C. D., Ingham, T., Larsen, N., Lewis, A. C., Liousse, C., Murphy, J. G., Orlandi, E., Oram, D. E.,
822 Saunois, M., Serça, D., Stewart, D. J., Stone, D., Thouret, V., Velthoven, P. van and Williams, J. E.: Atmospheric
823 composition of West Africa: Highlights from the AMMA international program, *Atmos. Sci. Lett.*, 12(1), 13–18,
824 doi:10.1002/asl.289, 2011.

825 Niedojadlo, A., Becker, K. H., Kurtenbach, R. and Wiesen, P.: The contribution of traffic and solvent use to the
826 total NMVOC emission in a German city derived from measurements and CMB modelling, *Atmos. Environ.*,
827 41(33), 7108–7126, doi:10.1016/j.atmosenv.2007.04.056, 2007.

828 Salameh, T., Afif, C., Sauvage, S., Borbon, A. and Locoge, N.: Speciation of non-methane hydrocarbons
829 (NMHCs) from anthropogenic sources in Beirut, Lebanon, *Environ. Sci. Pollut. Res.*, 21(18), 10867–10877,
830 doi:10.1007/s11356-014-2978-5, 2014.

831 Salameh, T., Sauvage, S., Afif, C., Borbon, A., Léonardis, T., Brioude, J., Waked, A. and Locoge, N.: Exploring
832 the seasonal NMHC distribution in an urban area of the Middle East during ECOCEM campaigns: Very high
833 loadings dominated by local emissions and dynamics, *Environ. Chem.*, 12(3), 316–328, doi:10.1071/EN14154,
834 2015.

835 Salameh, T., Borbon, A., Afif, C., Sauvage, S., Leonardis, T., Gaimoz, C. and Locoge, N.: Composition of gaseous
836 organic carbon during ECOCEM in Beirut, Lebanon: new observational constraints for VOC anthropogenic
837 emission evaluation in the Middle East, *Atmos. Chem. Phys. Discuss.*, (August), 1–32, doi:10.5194/acp-2016-
838 543, 2016a.

839 Salameh, T., Sauvage, S., Afif, C., Borbon, A. and Locoge, N.: Source apportionment vs. emission inventories of
840 non-methane hydrocarbons (NMHC) in an urban area of the Middle East: local and global perspectives, *Atmos.*
841 *Chem. Phys.*, 16(5), 3595–3607, doi:10.5194/acp-16-3595-2016, 2016b.

842 Saxton, J. E., Lewis, A. C., Kettlewell, J. H., Ozel, M. Z., Gogus, F., Boni, Y., Korogone, S. O. U. and Serça, D.:
843 Isoprene and monoterpene emissions from secondary forest in northern Benin, *Atmos. Chem. Phys. Discuss.*,
844 7(2), 4981–5012, doi:10.5194/acpd-7-4981-2007, 2007.

845 von Schneidmesser, E., Monks, P. S., Gros, V., Gauduin, J. and Sanchez, O.: How important is biogenic isoprene

846 in an urban environment? A study in London and Paris, *Geophys. Res. Lett.*, 38(19), doi:10.1029/2011GL048647,
847 2011.

848 Seinfeld, J. H. and Pandis, S. N.: *Atmospheric Chemistry and Physics. From Air Pollution to Climate Change*,
849 Second edi., John Wiley & Sons., 2006.

850 Sekimoto, K., Koss, A. R., Gilman, J. B., Selimovic, V., Coggon, M. M., Zarzana, K. J., Yuan, B., Lerner, B. M.,
851 Brown, S. S., Warneke, C., Yokelson, R. J., Roberts, J. M. and de Gouw, J.: High- and low-temperature pyrolysis
852 profiles describe volatile organic compound emissions from western US wildfire fuels, *Atmos. Chem. Phys.*
853 *Discuss.*, (February), 1–39, doi:10.5194/acp-2018-52, 2018.

854 SIE CI: Rapport Côte d'Ivoire Energie 2010., , 57 [online] Available from:
855 http://www.ecowrex.org/system/files/repository/2010_rapport_annuel_sie_-_min_ener.pdf (Accessed 27 August
856 2018), 2010.

857 Simpson, I. J., Akagi, S. K., Barletta, B., Blake, N. J., Choi, Y., Diskin, G. S., Fried, A., Fuelberg, H. E., Meinardi,
858 S., Rowland, F. S., Vay, S. A., Weinheimer, A. J., Wennberg, P. O., Wiebring, P., Wisthaler, A., Yang, M.,
859 Yokelson, R. J. and Blake, D. R.: Boreal forest fire emissions in fresh Canadian smoke plumes: C1-C10 volatile
860 organic compounds (VOCs), CO₂, CO, NO₂, NO, HCN and CH₃CN, *Atmos. Chem. Phys.*, 11(13), 6445–6463,
861 doi:10.5194/acp-11-6445-2011, 2011.

862 Sommariva, R., De Gouw, J. A., Trainer, M., Atlas, E., Goldan, P. D., Kuster, W. C., Warneke, C. and Fehsenfeld,
863 F. C.: Emissions and photochemistry of oxygenated VOCs in urban plumes in the Northeastern United States,
864 *Atmos. Chem. Phys.*, 11(14), 7081–7096, doi:10.5194/acp-11-7081-2011, 2011.

865 Sommers, W. T., Loehman, R. A. and Hardy, C. C.: Wildland fire emissions, carbon, and climate: Science
866 overview and knowledge needs, *For. Ecol. Manage.*, 317, 1–8, doi:10.1016/j.foreco.2013.12.014, 2014.

867 Stockwell, C. E., Veres, P. R., Williams, J. and Yokelson, R. J.: Characterization of biomass burning emissions
868 from cooking fires, peat, crop residue, and other fuels with high-resolution proton-transfer-reaction time-of-flight
869 mass spectrometry, *Atmos. Chem. Phys.*, 15(2), 845–865, doi:10.5194/acp-15-845-2015, 2015.

870 United Nations: *World Population Prospects: The 2017 Revision*, Dep. Econ. Soc. Aff. - Popul. Div., 2017.

871 Wang, M., Shao, M., Chen, W., Yuan, B., Lu, S., Zhang, Q., Zeng, L. and Wang, Q.: A temporally and spatially
872 resolved validation of emission inventories by measurements of ambient volatile organic compounds in Beijing,
873 China, *Atmos. Chem. Phys.*, 14(12), 5871–5891, doi:10.5194/acp-14-5871-2014, 2014.

874 Wang, Y. F., Owen, S. M., Li, Q. J. and Peñuelas, J.: Monoterpene emissions from rubber trees (*Hevea*
875 *brasiliensis*) in a changing landscape and climate: Chemical speciation and environmental control, *Glob. Chang.*
876 *Biol.*, 13(11), 2270–2282, doi:10.1111/j.1365-2486.2007.01441.x, 2007.

877 Warneke, C., Trainer, M., de Gouw, J. A., Parrish, D. D., Fahey, D. W., Ravishankara, A. R., Middlebrook, A.
878 M., Brock, C. A., Roberts, J. M., Brown, S. S., Neuman, J. A., Lerner, B. M., Lack, D., Law, D., Hübler, G.,
879 Pollack, I., Sjostedt, S., Ryerson, T. B., Gilman, J. B., Liao, J., Holloway, J., Peischl, J., Nowak, J. B., Aikin, K.
880 C., Min, K.-E., Washenfelder, R. A., Graus, M. G., Richardson, M., Markovic, M. Z., Wagner, N. L., Welti, A.,
881 Veres, P. R., Edwards, P., Schwarz, J. P., Gordon, T., Dube, W. P., McKeen, S. A., Brioude, J., Ahmadov, R.,

882 Bougiatioti, A., Lin, J. J., Nenes, A., Wolfe, G. M., Hanisco, T. F., Lee, B. H., Lopez-Hilfiker, F. D., Thornton,
883 J. A., Keutsch, F. N., Kaiser, J., Mao, J. and Hatch, C. D.: Instrumentation and measurement strategy for the
884 NOAA SENEX aircraft campaign as part of the Southeast Atmosphere Study 2013, *Atmos. Meas. Tech.*, 9(7),
885 3063–3093, doi:10.5194/amt-9-3063-2016, 2016.

886 Wiedinmyer, C., Yokelson, R. J. and Gullett, B. K.: Global Emissions of Trace Gases, Particulate Matter, and
887 Hazardous Air Pollutants from Open Burning of Domestic Waste, *Environ. Sci. Technol.*, 48(16), 9523–9530,
888 doi:10.1021/es502250z, 2014.

889 Yokelson, R. J., Burling, I. R., Gilman, J. B., Warneke, C., Stockwell, C. E., De Gouw, J., Akagi, S. K., Urbanski,
890 S. P., Veres, P., Roberts, J. M., Kuster, W. C., Reardon, J., Griffith, D. W. T., Johnson, T. J., Hosseini, S., Miller,
891 J. W., Cocker, D. R., Jung, H. and Weise, D. R.: Coupling field and laboratory measurements to estimate the
892 emission factors of identified and unidentified trace gases for prescribed fires, *Atmos. Chem. Phys.*, 13(1), 89–
893 116, doi:10.5194/acp-13-89-2013, 2013.

894 Zhang, Q., Yuan, B., Shao, M., Wang, X., Lu, S., Lu, K., Wang, M., Chen, L., Chang, C. C. and Liu, S. C.:
895 Variations of ground-level O₃ and its precursors in Beijing in summertime between 2005 and 2011, *Atmos. Chem.*
896 *Phys.*, 14(12), 6089–6101, doi:10.5194/acp-14-6089-2014, 2014.

897

898

899 **List of figures**

900 **Figure 1.** Geographical location of Abidjan, Côte d'Ivoire and spatial distribution of ambient VOC measurements. Red stars
901 indicate the VOC measurement sites and the blue square represents the meteorology site. More information about the ambient
902 site is detailed in Table 2.

903 **Figure 2.** Meteorological data observed in Abidjan, Côte d'Ivoire. The figure represents a) the weekly accumulated
904 precipitation (in mm month⁻¹) and weekly mean air temperature (in °C) and b) the wind speed (in m s⁻¹) and direction observed
905 (deg), during the field campaigns (2016). Data was downloaded from the National Centers for environmental information
906 site (NCDC), NOAA and recorded at Abidjan International Airport (see location in Figure 1).

907 **Figure 3.** Spatial distribution of VOCs measured at ambient sites in Abidjan, size-coded by the sum of VOCs (in µg m⁻³) and
908 color-coded by the relative contribution of BTEX compounds, namely benzene (Benz), toluene (Tol), ethylbenzene (EthylB),
909 m+p-xylene (m+p-xyl) and o-xylene (o-xyl). Values shown in each pie-chart represent the total VOC concentration measured
910 at the sampling point. Ambient site names and characteristics are presented in Table 2.

911 **Figure 4.** Boxplot showing the VOC concentrations (µg m⁻³) at Abidjan ambient sites (upper panel). The middle line in each
912 box plot indicates the median (50th percentile), the lower and upper box limits represent the 25th and 75th quartiles,
913 respectively, and the whiskers the 99% coverage assuming the data has a normal distribution. The lower panel shows the
914 mean concentrations reported in other cities worldwide, such as Abidjan (this study), Paris (AIRPARIF, 2013), São Paulo
915 (Dominutti et al., 2016), Beirut (Salameh et al., 2014), Karachi (Barletta et al., 2002) and South Africa (Jaars et al., 2014).

916 **Figure 5.** Relative concentration comparison between ambient measurements and emission source profiles of VOCs
917 measured in Abidjan, Côte d'Ivoire. Orange and yellow based colours represent the contributions of alkanes, blue based
918 colours aromatics, and green-based colours terpenes and isoprene.

919 **Figure 6.** Contribution of VOC reported in table S1 to the measured molar mass of anthropogenic sources analysed in
920 Abidjan, aggregated in VOC families (table S2). The emission sources under analysis are heavy-duty diesel vehicles
921 (HDDV), two-wheel two-stroke vehicles (TW2T), two-wheel four-stroke vehicles (TW4T), light-duty diesel vehicles
922 (LDDV), light-duty gasoline vehicles (LDGV), charcoal burning (CH), fuelwood burning (FW), charcoal making (CHM)
923 and landfill waste burning (WB). Values in the upper panel represent the total measured molar mass (in µg cm⁻³ ppm CO⁻¹)
924 of the respective anthropogenic source.

925 **Figure 7.** Contributions of VOC emission ratios to (a)–(d) the measured molar mass, (e)–(h) OH reactivity, (i)–(l) relative
926 ozone formation potential POCP and (m)–(p) relative SOA formation potential, aggregated in VOC families. Absolute totals
927 for each source are shown below each pie chart in the respective units.

928 **Figure 8.** Comparison of VOC emission profiles for Côte d'Ivoire from the emissions estimated from the measurements of
929 this study (Keita et al., 2018) and the EDGAR v4.3.2 (Huang et al., 2017) and MACCity inventories (Granier et al., 2011).
930 The profile analysis integrates road transportation and residential sectors based on the sector activity for 2012. a) absolute
931 emissions, in Tg year⁻¹, b) relative mass contribution, and c) relative mass reactivity, considering 100 Tg of emissions
932 weighted by the kOH reaction rate calculated for each VOC family.

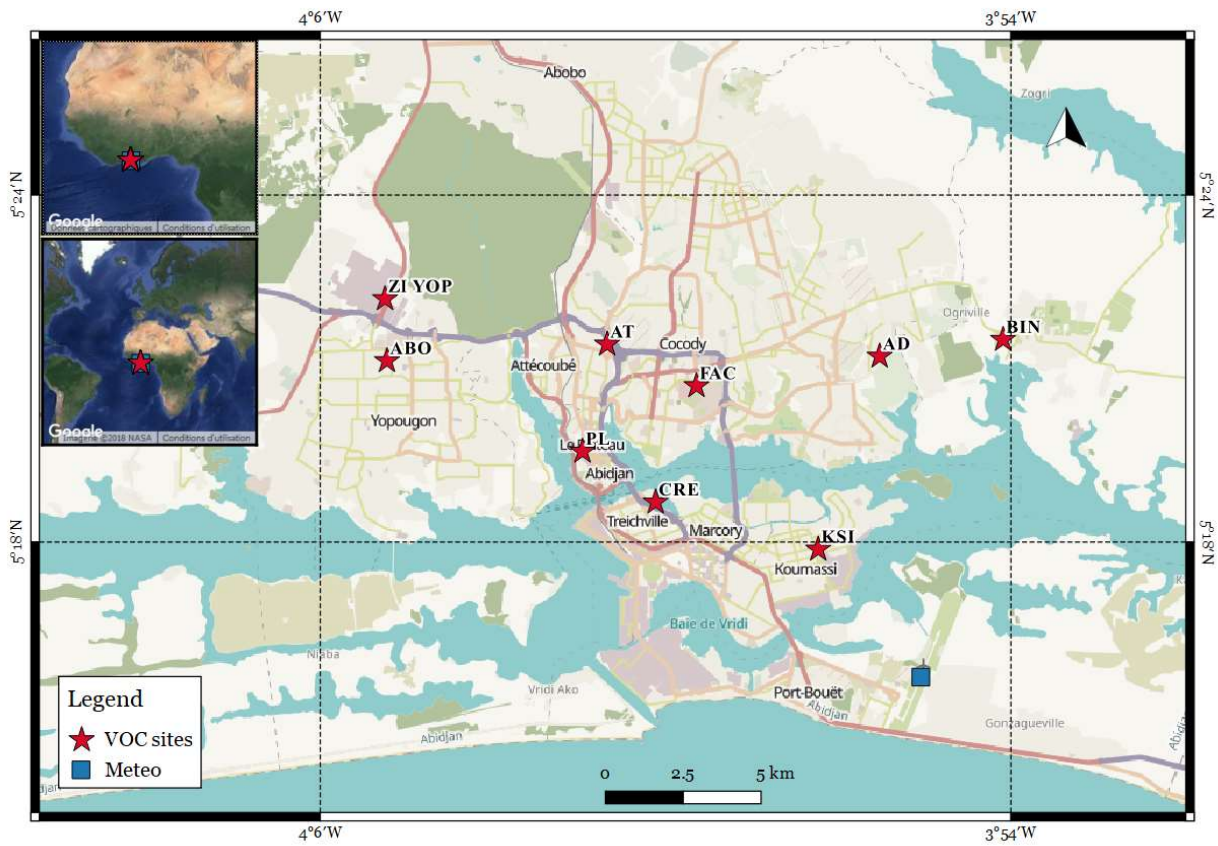
933 **Figure 9.** VOC emission profiles considering all the VOC families calculated from the measurements of our study and
934 compared with the global EDGAR v4.3.2 inventory (Huang et al., 2017). The comparison integrates road transportation (RT)
935 and residential (Resid) sectors in Côte d'Ivoire and Europe for the year 2012. Absolute emissions are expressed in Gg year⁻¹
936 for each VOC group.

937 **Figure 10.** Total estimated emissions and relative distributions in the anthropogenic sources measured in Côte d'Ivoire for
938 the VOC family a) Terpenes, b) IVOCs and c) Aldehydes.

939 **Figure 11.** Distribution of monoterpenes and isoprene in the emission sources measured in Abidjan. The values represent the
940 percentage of each biogenic VOC over the total emission estimated for these species.

941

942

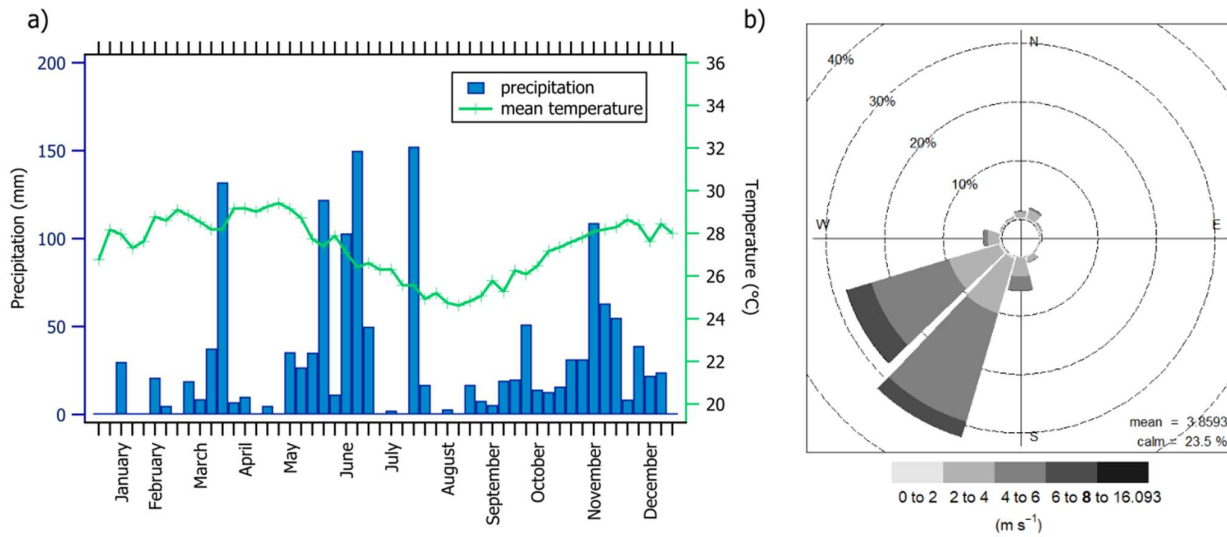


943

944 **Figure 1.** Geographical location of Abidjan, Côte d'Ivoire and spatial distribution of ambient VOC measurements.

945 Red stars indicate the VOC measurement sites and the blue square represents the meteorology site. More
 946 information about the ambient site is detailed in Table 2.

947

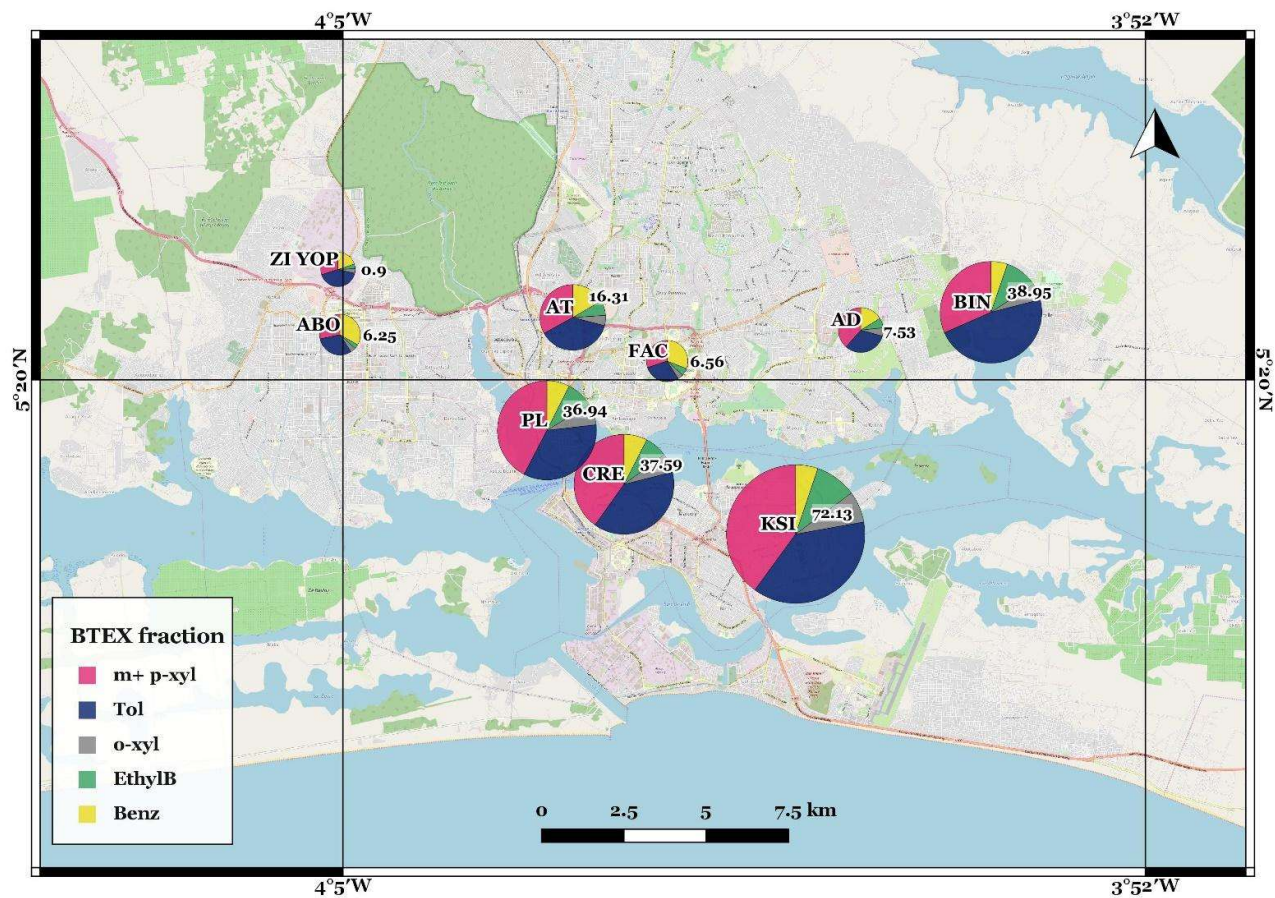


948

949

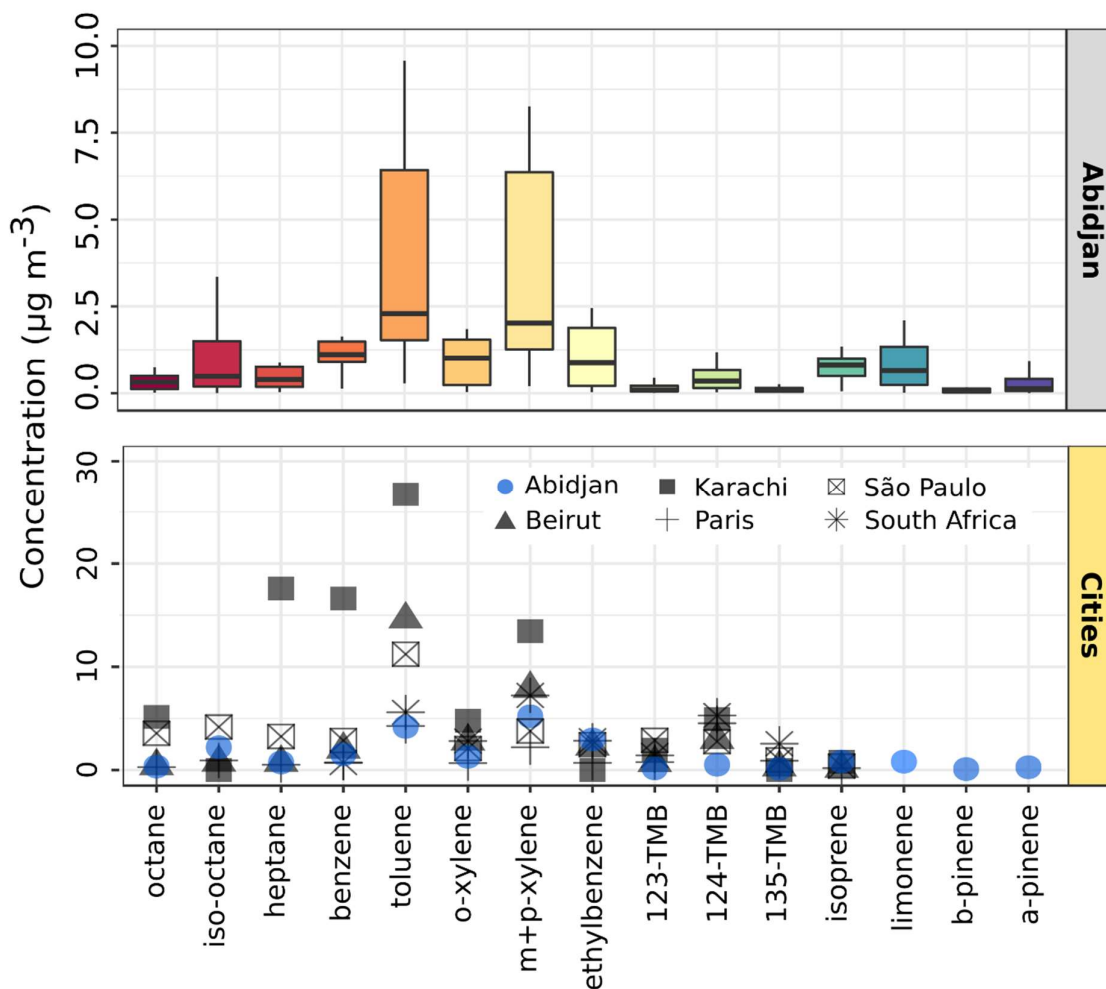
950 **Figure 2.** Meteorological data observed in Abidjan, Côte d'Ivoire. The figure represents a) the weekly
 951 accumulated precipitation (in mm month⁻¹) and weekly mean air temperature (in °C) and b) the wind speed (in m
 952 s⁻¹) and direction observed (deg), during the field campaigns (2016). Data was downloaded from the National
 953 Centers for environmental information site (NCDC), NOAA and recorded at Abidjan International Airport (see
 954 location in Figure 1).

955



956
 957
 958
 959
 960
 961
 962
 963

Figure 3. Spatial distribution of VOCs measured at ambient sites in Abidjan, size-coded by the sum of VOCs (in $\mu\text{g m}^{-3}$) and color-coded by the relative contribution of BTEX compounds, namely benzene (Benz), toluene (Tol), ethylbenzene (EthylB), m+p-xylene (m+p-xyl) and o-xylene (o-xyl). Values shown in each pie-chart represent the total VOC concentration measured at the sampling point. Ambient site names and characteristics are presented in Table 2.

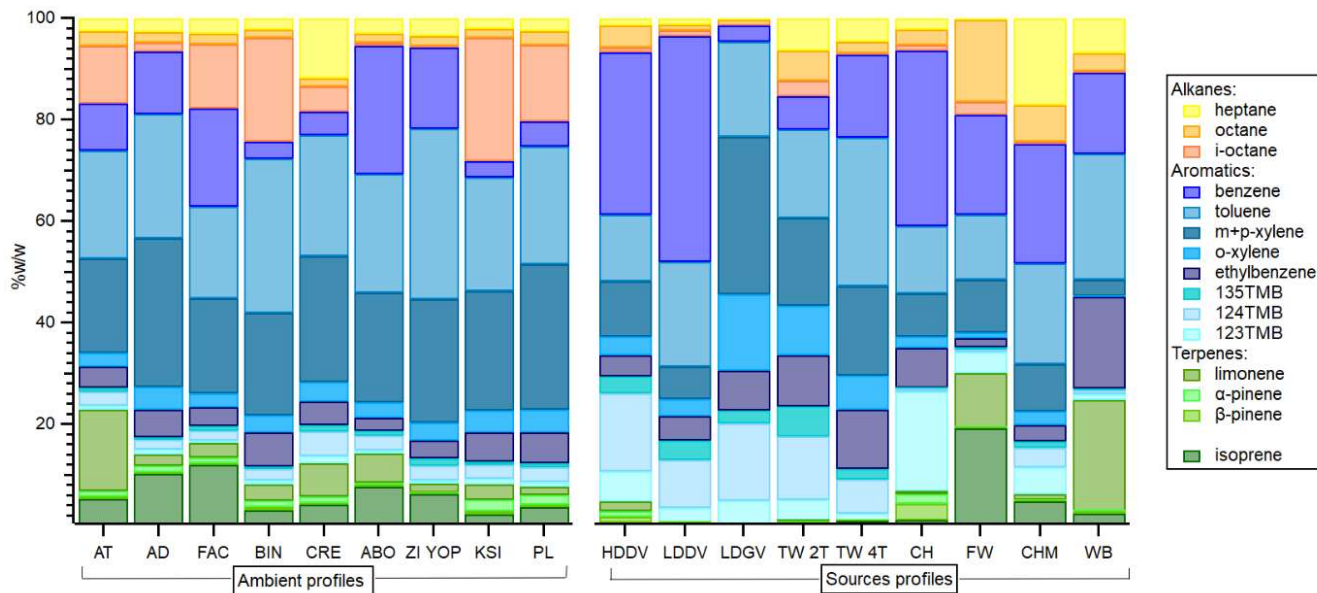


964

965

966 **Figure 4.** Boxplot showing the VOC concentrations ($\mu\text{g m}^{-3}$) at Abidjan ambient sites (upper panel). The middle
 967 line in each box plot indicates the median (50th percentile), the lower and upper box limits represent the 25th and
 968 75th quartiles, respectively, and the whiskers the 99% coverage assuming the data has a normal distribution. The
 969 lower panel shows the mean concentrations reported in other cities worldwide, such as Abidjan (this study), Paris
 970 (AIRPARIF, 2013), São Paulo (Dominutti et al., 2016), Beirut (Salameh et al., 2014), Karachi (Barletta et al.,
 971 2002) and South Africa (Jaars et al., 2014).

972



974

975 **Figure 5.** Relative concentration comparison between ambient measurements and emission source profiles of
 976 VOCs measured in Abidjan, Côte d'Ivoire. Orange and yellow based colours represent the contributions of
 977 alkanes, blue based colours aromatics, and green-based colours terpenes and isoprene.

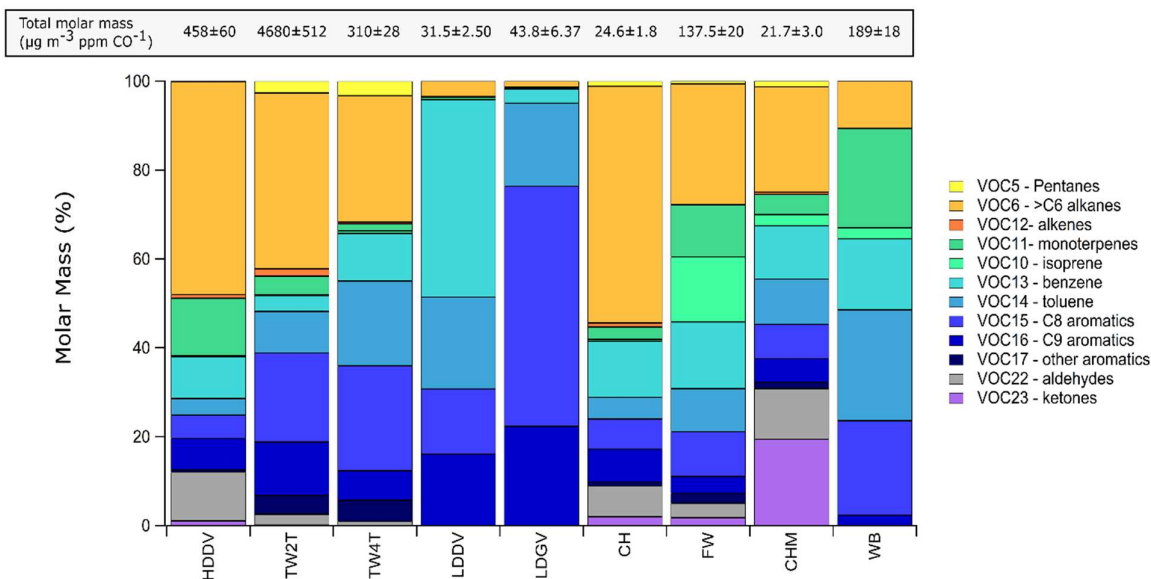
978

979

980

981

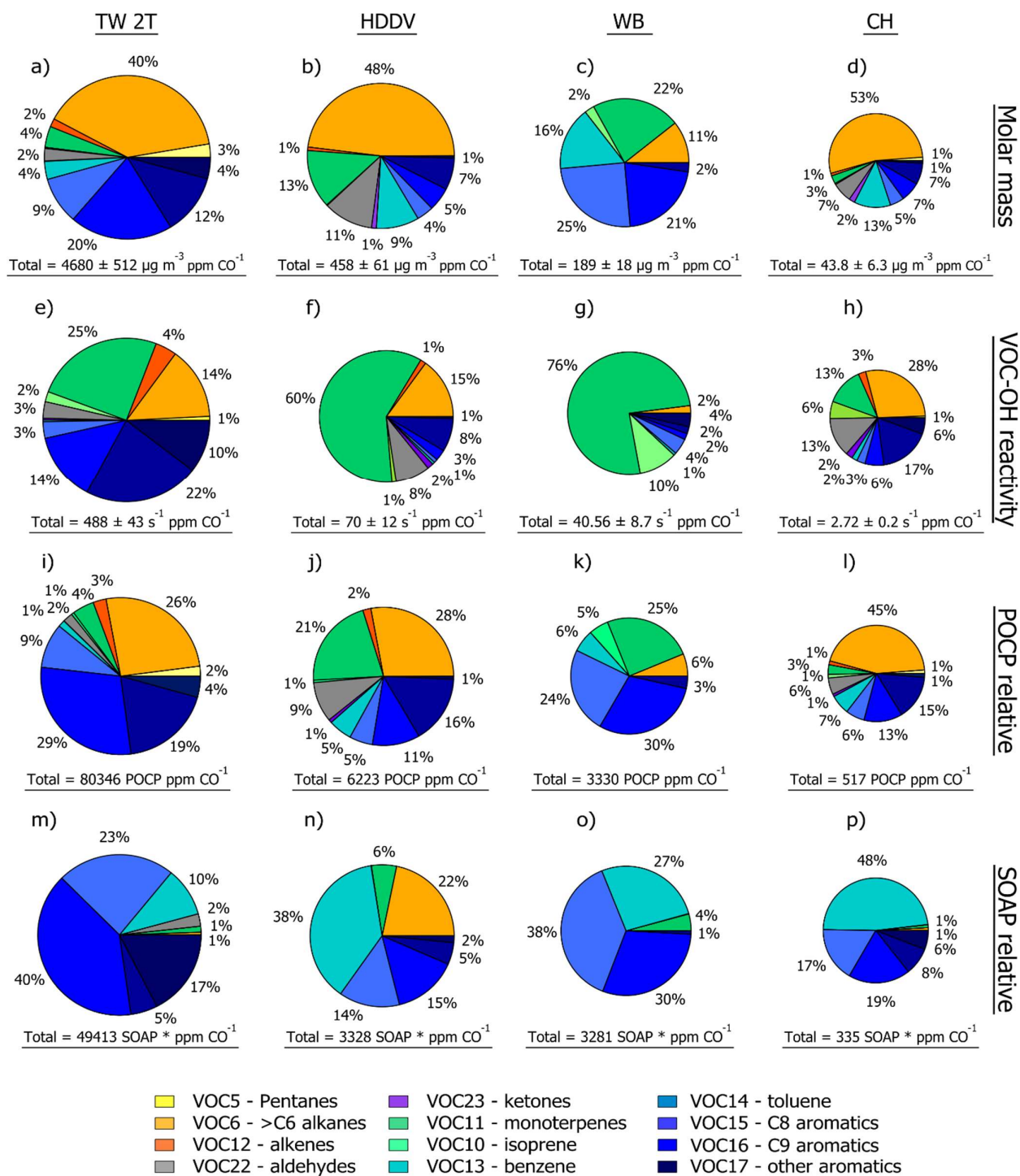
982



983

984 **Figure 6.** Contribution of VOC reported in table S1 to the measured molar mass of anthropogenic sources
985 analysed in Abidjan, aggregated in VOC families (table S2). The emission sources under analysis are heavy-duty
986 diesel vehicles (HDDV), two-wheel two-stroke vehicles (TW2T), two-wheel four-stroke vehicles (TW4T), light-
987 duty diesel vehicles (LDDV), light-duty gasoline vehicles (LDGV), charcoal burning (CH), fuelwood burning
988 (FW), charcoal making (CHM) and landfill waste burning (WB). Values in the upper panel represent the total
989 measured molar mass (in $\mu\text{g cm}^{-3}$ ppm CO^{-1}) of the respective anthropogenic source.

990

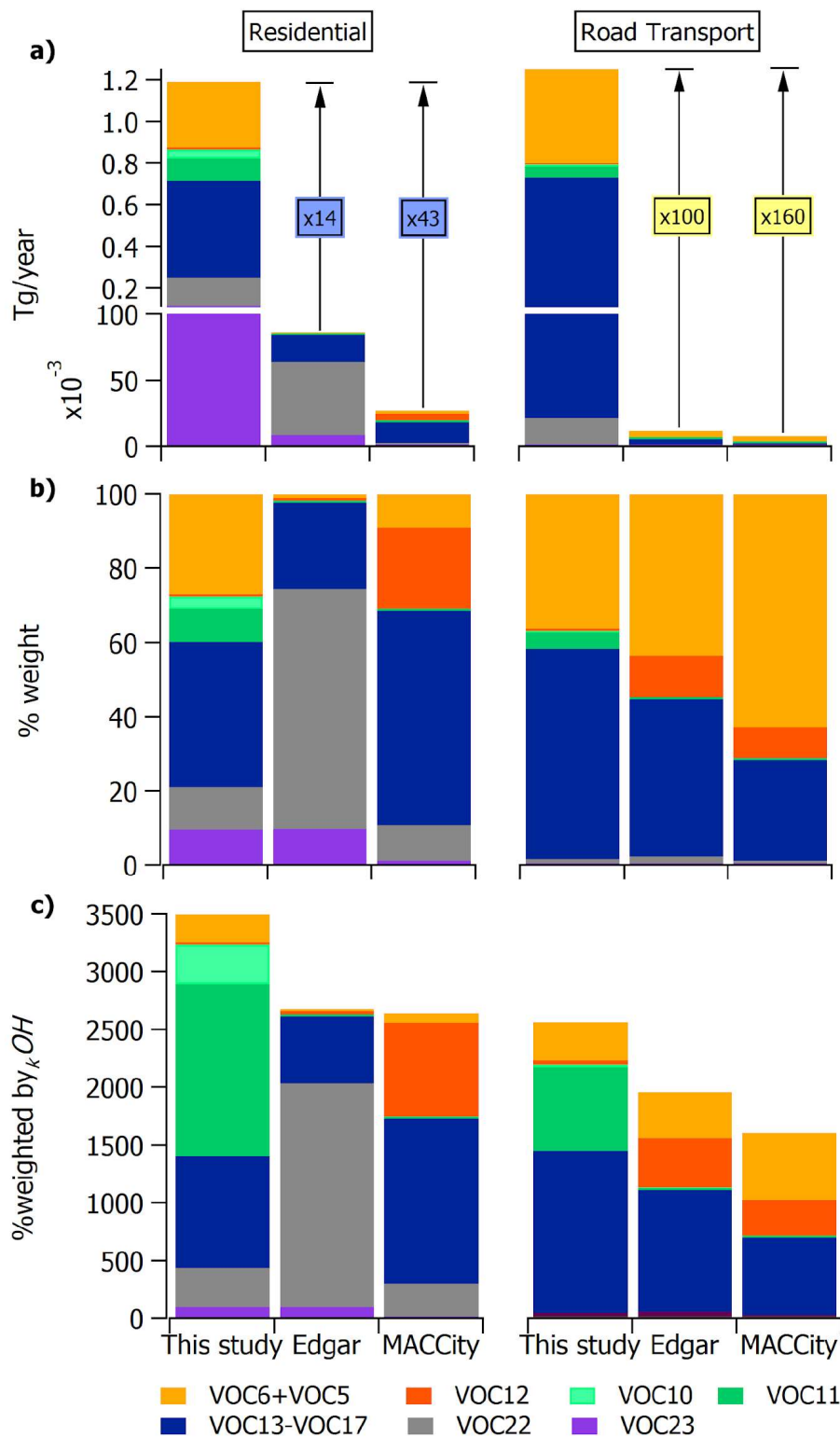


993

994 **Figure 7.** Contributions of VOC emission ratios to (a)–(d) the measured molar mass, (e)–(h) OH reactivity, (i)–
 995 (l) relative ozone formation potential POCP and (m)–(p) relative SOA formation potential, aggregated in VOC
 996 families. Absolute totals for each source are shown below each pie chart in the respective units.

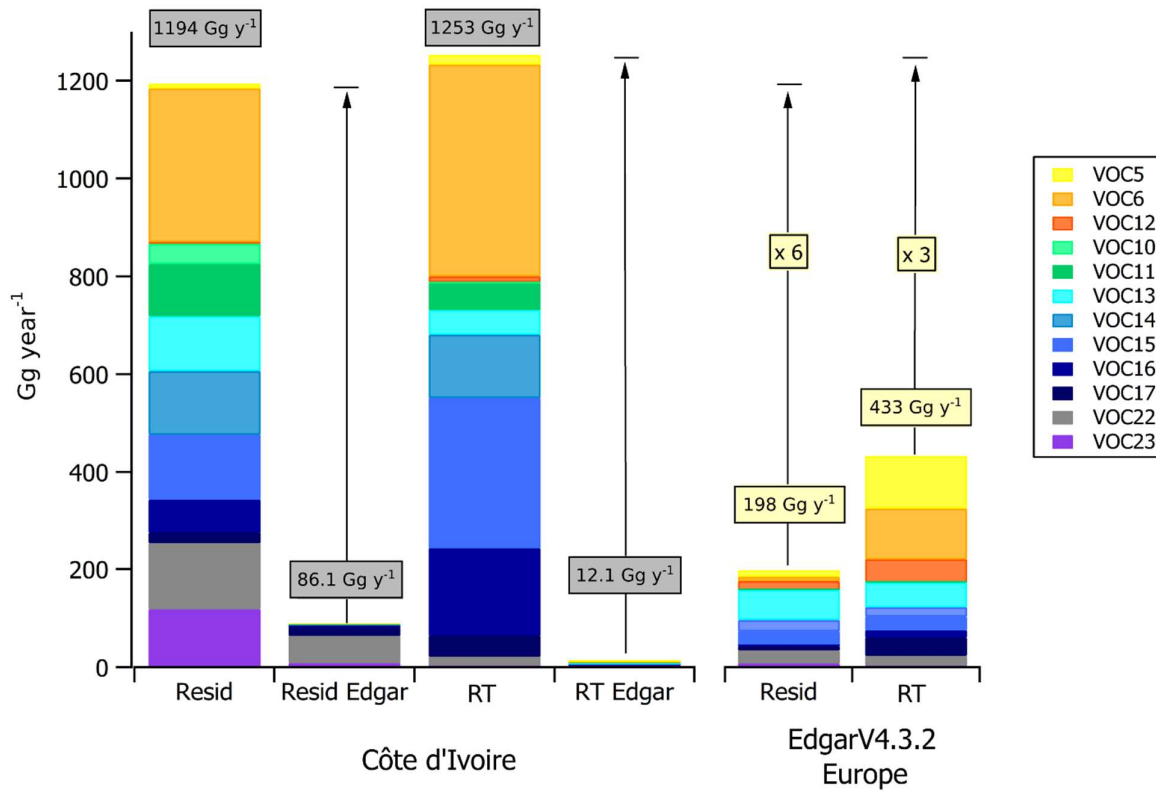
997

998



999

1000 **Figure 8.** Comparison of VOC emission profiles for Côte d'Ivoire from the emissions estimated from the
 1001 measurements of this study (Keita et al., 2018) and the EDGAR v4.3.2 (Huang et al., 2017) and MACCity
 1002 inventories (Granier et al., 2011). The profile analysis integrates road transportation and residential sectors based
 1003 on the sector activity for 2012. a) absolute emissions, in Tg year⁻¹, b) relative mass contribution, and c) relative
 1004 mass reactivity, considering 100 Tg of emissions weighted by the kOH reaction rate calculated for each VOC
 1005 family.



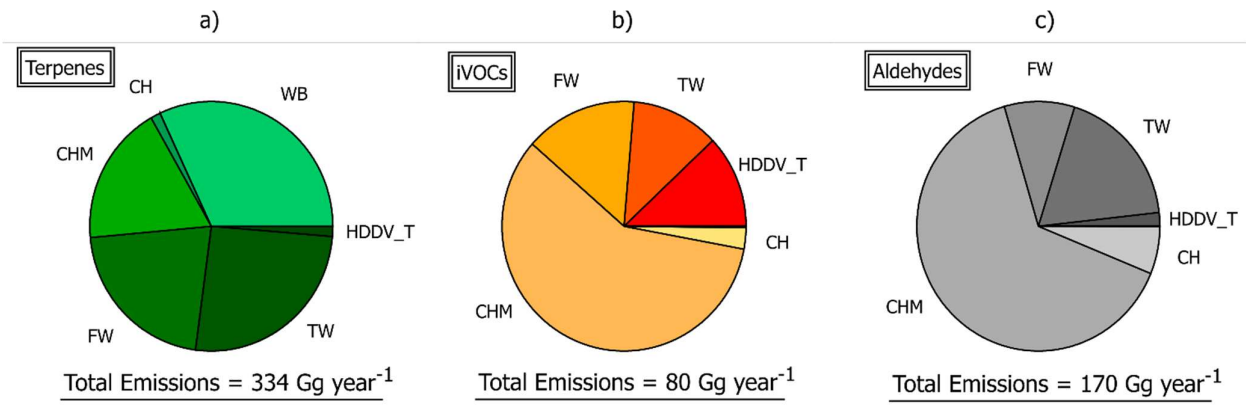
1007

1008 **Figure 9.** VOC emission profiles considering all the VOC families calculated from the measurements of our study
 1009 and compared with the global EDGAR v4.3.2 inventory (Huang et al., 2017). The comparison integrates road
 1010 transportation (RT) and residential (Resid) sectors in Côte d'Ivoire and Europe for the year 2012. Absolute
 1011 emissions are expressed in Gg year⁻¹ for each VOC group.

1012

1013

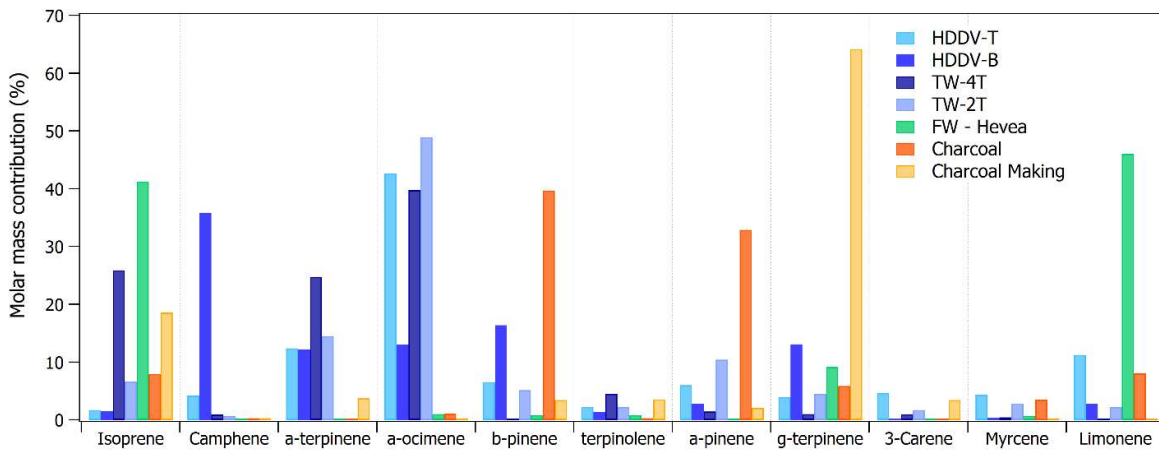
1014



1015

1016 **Figure 10.** Total estimated emissions and relative distributions in the anthropogenic sources measured in Côte
1017 d'Ivoire for the VOC family a) Terpenes, b) IVOCs and c) Aldehydes.

1018



1019

1020 **Figure 11.** Distribution of monoterpenes and isoprene in the emission sources measured in Abidjan. The values
 1021 represent the percentage of each biogenic VOC over the total emission estimated for these species.

1022

1023

1024
1025
1026
1027
1028
1029
1030
1031

List of Tables

Table 1. Description of the emission sources measured and evaluated in Abidjan, Côte d'Ivoire.
Table 2. Geographical location and characteristics of ambient measurement sites in Abidjan, Côte d'Ivoire

Table 1. Description of the emission sources measured and evaluated in Abidjan, Côte d'Ivoire.

Reference	Sub-group	Description	source	type
HDDV		Heavy-duty diesel vehicles	Diesel emissions	Road Transport
	HDDV-T	Diesel trucks	Diesel emissions	Road Transport
	HDDV-B	Diesel buses	Diesel emissions	Road Transport
LDDV		Light-duty diesel vehicles	Diesel emissions	Road Transport
LDGV		Light-duty gasoline vehicles	Gasoline emissions	Road Transport
TW	TW2T	Two-wheel two-stroke	a mixture of smuggled oil and gasoline	Road Transport
	TW4T	Two-wheel four-stroke	a mixture of smuggled oil and gasoline	Road Transport
CH		Charcoal	Charcoal burning	Residential
FW		Fuelwood burning	<i>Hevea brasiliensis</i>	Residential
CHM		Charcoal making	Charcoal fabrication	Residential
WB		Waste burning	Domestic landfill burning	Waste burning

1036

1037

1038

Table 2. Geographical location and characteristics of ambient measurement sites in Abidjan, Côte d'Ivoire

ID	Site location	Longitude	Latitude	Activity
AT	Adjame	04°01'04"W	05°21'14"N	Traffic site A site near a transport station; regular traffic jams, ancient public transport vehicles
AD	Akouédo	03°56'16"W	05°21'12"N	Landfill- waste burning Uncontrolled landfill, continuous waste burning
FAC	Cocody	03°59'27"W	05°20'42"N	Residential University residence
BIN	Bingerville	03°54'07"W	05°21'30"N	Urban Background Far from traffic, near to Ebrié Lagoon
CRE	Treichville	04°00'10"W	05°18'41"N	Green urban area Near to Ebrié Lagoon; much wind Traffic + residential
ABO	Abobo	04°04'10"W	05°26'08"N	Townhall, near to the big market of Abobo. Old communal taxis and minibuses in a crowded crossroad, human activities Industrial area
ZI YOP	Yopougon	04°04'52"W	05°22'12"N	All type of industries (cement, agro-industries, plastic and iron processing, pharmaceutical and cosmetics); heavy-duty vehicles and traffic jams Domestic fires + traffic
KSI	Koumassi	03°57'20"W	05°17'52"N	A residential site mainly influenced by domestic activities, fire-wood, and charcoal; old vehicles Traffic/ administrative
PL	Plateau	04°01'26"W	05°19'33"N	City center, crossroad with traffic jams; Light-duty vehicles, near the train station

1039

1040